

1     **Deep learning-based networks for automated recognition and classification of awkward**  
2             **working postures in construction using wearable insole sensor data**

3             Maxwell Fordjour ANTWI-AFARI<sup>a\*</sup>, Yazan QAROUT<sup>b</sup>, Randa HERZALLAH<sup>c</sup>, Shahnawaz  
4                     ANWER<sup>d</sup>, Waleed UMER<sup>e</sup>, Yongcheng ZHANG<sup>f</sup>, Patrick MANU<sup>g</sup>

5     <sup>a</sup>Lecturer, Department of Civil Engineering, College of Engineering and Physical Sciences, Aston  
6     University, Birmingham, B4 7ET, United Kingdom. Email: [m.antwifari@aston.ac.uk](mailto:m.antwifari@aston.ac.uk)

7  
8     <sup>b</sup>Informatics, The Manufacturing Technology Centre Ltd, Ansty Park, Coventry, CV7 9JU, United  
9     Kingdom. Email: [yazan.qarout@gmail.com](mailto:yazan.qarout@gmail.com)

10  
11    <sup>c</sup>Reader, Systems Analytics Research Institute, Aston University, Aston Triangle, Birmingham,  
12    B4 7ET, United Kingdom. Email: [r.herzallah@aston.ac.uk](mailto:r.herzallah@aston.ac.uk)

13  
14    <sup>d</sup>Postdoctoral Research Fellow, Department of Building and Real Estate, The Hong Kong  
15    Polytechnic University, Room No. ZN1002, Hung Hom, Kowloon, Hong Kong Special  
16    Administrative Region. E-mail: [shahnawaz.anwer@connect.polyu.hk](mailto:shahnawaz.anwer@connect.polyu.hk)

17  
18    <sup>e</sup>Senior Lecturer, Department of Mechanical and Construction Engineering, Northumbria  
19    University, NE7 7YT, Newcastle upon Tyne, United Kingdom. Email:  
20    [waleed.umer@northumbria.ac.uk](mailto:waleed.umer@northumbria.ac.uk)

21  
22    <sup>f</sup>Lecturer, Department of Construction Management, Huaiyin Institute of Technology, Huaian,  
23    223003, China. Email: [cquzhych@hyit.edu.cn](mailto:cquzhych@hyit.edu.cn)

24  
25    <sup>g</sup>Reader, Department of Mechanical, Aerospace and Civil Engineering, The University of  
26    Manchester, M13 9LP, Manchester, United Kingdom. Email: [Patrick.Manu@manchester.ac.uk](mailto:Patrick.Manu@manchester.ac.uk)

27  
28  
29    **\*Corresponding author:**

30    Lecturer, Department of Civil Engineering, College of Engineering and Physical Sciences, Aston  
31    University, Birmingham, B4 7ET, United Kingdom. Email: [m.antwifari@aston.ac.uk](mailto:m.antwifari@aston.ac.uk)

32 **Abstract**

33 Among the numerous work-related risk factors, construction workers are often exposed to  
34 awkward working postures that may lead them to develop work-related musculoskeletal disorders  
35 (WMSDs). To mitigate WMSDs among construction workers, awkward working posture  
36 recognition is the first step in proactive WMSD prevention. Several researchers have proposed  
37 wearable sensor-based systems and machine learning classifiers for awkward posture recognition.  
38 However, these wearable sensor-based systems (e.g., surface electromyography) are either  
39 intrusive or require attaching multiple sensors on workers' bodies, which may lead workers'  
40 discomfort and systemic instability, thus, limiting their application on construction sites. In  
41 addition, machine learning classifiers are limited to human-specific shallow features which  
42 influence model performance. To address these limitations, this study proposes a novel approach  
43 by using wearable insole pressure system and recurrent neural network (RNN) models, which  
44 automate feature extraction and are widely used for sequential data classification. Therefore, the  
45 research objective is to automatically recognize and classify different types of awkward working  
46 postures in construction by using deep learning-based networks and wearable insole sensor data.  
47 The classification performance of three RNN-based deep learning models, namely: (1) long-short  
48 term memory (LSTM), (2) bidirectional LSTM (Bi-LSTM), and (3) gated recurrent units (GRU),  
49 was evaluated using plantar pressure data captured by a wearable insole system from workers on  
50 construction sites. The experimental results show that GRU model outperforms the other RNN-  
51 based deep learning models with a high accuracy of 99.01% and F1-score between 93.19% and  
52 99.39%. These results demonstrate that GRU models can be employed to learn sequential plantar  
53 pressure patterns captured by a wearable insole system to recognize and classify different types of  
54 awkward working postures. The findings of this study contribute to wearable sensor-based posture-  
55 related recognition and classification, thus, enhancing construction workers' health and safety.

56

57 **Keywords:** Awkward working postures; Deep learning networks; Wearable insole pressure  
58 system, Work-related musculoskeletal disorders, Work-related risk recognition.

59 **1. Introduction**

60 The construction industry suffers from numerous health and safety problems because construction  
61 activities involve diverse resources and physically demanding tasks. In Australia, there were 26  
62 out of 183 fatalities in the construction industry in 2019, which accounted for a 2.2 fatality rate  
63 (fatalities per 100,000 workers) across all industries (Safety Work Australia, 2020). Among  
64 construction-related health and safety problems, work-related musculoskeletal disorders (WMSDs)  
65 are the leading cause of non-fatal occupational injuries (Umer et al., 2017a; Anwer et al., 2021;  
66 Anwer et al., 2021). WMSDs refer to a wide range of injuries or disorders that result in pain and/or  
67 other sensations in the muscles, nerves, tendons, ligaments, and joints (Wang et al., 2015a).  
68 Examples of WMSDs include low back disorders, carpal tunnel syndrome, tendonitis, and bursitis  
69 (Umer et al., 2017a; Antwi-Afari et al., 2018a). According to the Health and Safety Executive  
70 (HSE) in the UK, WMSDs accounted for 57% of 81,000 work-related ill health cases injuries  
71 (HSE, 2020). Gibb et al. (2018) estimated that in the UK, WMSDs costs construction employers  
72 about GBP 650 million/year out of a total estimated burden of occupational ill-health cost of about  
73 GBP 850 million/year. Given that WMSDs still remain a health and safety problem in construction,  
74 there is an urgent need to recognize work-related risk factors that may lead workers to develop  
75 WMSDs.

76  
77 The high prevalence rate of WMSDs among construction workers could be attributed to several  
78 work-related physical risk factors, psychosocial stressors, and individual factors (Wang et al.,  
79 2015a; Umer et al., 2017b). Taken together, they can lead to work absenteeism, schedule delays,  
80 increased cost of medical expenses, loss of income and productivity, and early retirement (Umer  
81 et al., 2017a; Yu et al., 2021). Examples of work-related risk factors include repetitive motions,

82 gender, age, safety concerns, overexertion, awkward working posture, and poor working  
83 conditions such as high vibration, and extreme temperature (Wang et al., 2015a; Umer et al., 2020;  
84 Anwer et al., 2021; Yu et al., 2021). Among the various work-related risk factors, awkward  
85 working postures (e.g., stoop, squat) are the major risk factor that causes WMSDs in construction.  
86 According to the Center for Construction Research and Training (CPWR), roofers and painters are  
87 on their knees, crouching or stooping more than 60% of the time, and brick masons spend 93% of  
88 their time bending and twisting their bodies (CPWR, 2018). Consequently, research on automated  
89 recognition of awkward working postures has become relevant to both researchers and  
90 practitioners in developing proactive interventions which could aid WMSDs risk factors  
91 prevention in construction.

92  
93 Generally, one of the critical steps to mitigate WMSDs risk factors is to identify an ergonomic risk  
94 approach for recognizing a potential work-related risk factor. In the past decades, work-related  
95 risk factors were mainly recognized by using ergonomic risk approaches such as observation-based  
96 methods (McAtamney and Corlett, 1993; Hignett and McAtamney, 2000). Although these  
97 traditional ergonomic risk approaches are simple and less expensive, they mostly involve  
98 subjective judgments and a large amount of manual data which make them time-consuming, and  
99 error-prone (David, 2005). Alternatively, wearable sensing technologies have been developed to  
100 monitor and recognize work-related risk factors effectively, thus preventing WMSDs (Antwi-Afari  
101 et al., 2019a). Among them, wearable inertial measurement units (WIMUs) have been widely used  
102 for automated recognition and classification of awkward working postures among construction  
103 workers (Chen et al., 2017; Valero et al., 2017; Lee et al., 2020). WIMUs-based systems collect  
104 acceleration, angular velocity, and geomagnetic field measurements of a worker's bodily

105 movements, which are used to automatically monitor awkward working postures (Chen et al., 2017;  
106 Valero et al., 2017). However, attaching multiple WIMUs-based systems on different body parts  
107 not only significantly intrude a worker's task, but also often causes synchronization issues, body  
108 discomfort, and sensor stream deviations due to varying sensor locations (Guo et al., 2017).

109

110 In recent years, research works on automated recognition and classification of work-related risk  
111 factors have demonstrated the application of computational techniques such as machine learning  
112 classifiers to train and evaluate classifier performance (Akhavian and Behzadan, 2016; Nath et al.,  
113 2018; Ryu et al., 2019; Antwi-Afari et al., 2020a; Umer et al., 2020). Even though these studies  
114 have shown promising results, traditional machine learning classifiers implement pattern  
115 recognition approaches. These approaches require multiple pre-processing steps such as manual  
116 segmentation of continuous time-series sensor data with different window sizes, and further  
117 extraction of statistically significant feature vectors, which are inefficient and time-consuming  
118 (Portugal et al., 2018). In addition, the use of human-specific shallow features leads to poor  
119 performance in incremental learning. Moreover, traditional machine learning classifiers treat each  
120 time step of the time-series sensor data as statistically independent, thus, ignoring the temporal  
121 relationship between consecutive time steps (Rashid and Louis, 2019). These limitations of  
122 traditional machine learning classifiers motivate this current research to use deep learning  
123 networks to automatically extract relevant features with spatio-temporal dependency captured by  
124 a wearable insole pressure system.

125

126 To date, the literature mostly focuses on WIMUs-based systems and machine learning applications  
127 for automated recognition and classification of work-related risk factors. Although they provided  
128 useful evidence for mitigating WMSD risk factors among construction workers, they were limited

129 due to attaching intrusive wearable sensor-based systems and adopting machine learning classifiers  
130 that use hand-crafted feature extraction methods for model evaluation. To address these limitations,  
131 the present study proposed a non-intrusive wearable insole sensor system, which was used to  
132 collect plantar pressure data and deep learning-based networks for classification performance.  
133 Therefore, the objective of this research was to evaluate a novel approach of using deep learning-  
134 based networks and wearable insole sensor data to automatically recognize and classify different  
135 types of awkward working postures in construction. Consequently, the current study adopted  
136 recurrent neural networks (RNNs), deep learning models to train time-series plantar pressure data  
137 captured by a wearable insole pressure sensor. In this study, plantar pressure data were collected  
138 from a construction site when construction workers performed several awkward working postures  
139 (i.e., overhead working, squatting, stooping, semi-squatting, and one-legged kneeling) during their  
140 daily activities. In the context of a real construction site experiment, it was hypothesized that the  
141 proposed approach could produce reliable and better performance accuracy for classifying  
142 different types of awkward working postures. The findings of this study could not only  
143 complement existing wearable sensor-based systems used for work-related risk factors recognition  
144 but also provide a novel method that could be beneficial to both researchers and safety managers  
145 to mitigate WMSDs risk factors in construction.

146

## 147 **2. Research Background**

148 This section mainly presents existing research studies related to ergonomic risk approaches for  
149 recognizing work-related risk factors. In addition, extant literature on wearable sensor-based  
150 systems for automated recognition and WMSDs prevention are thoroughly discussed. Lastly, the

151 feasibility of using wearable insole sensor data and deep learning network-based classification in  
152 construction is discussed.

153

### 154 *2.1. Ergonomic risk approaches for recognizing work-related risk factors*

155 To mitigate the risk of developing WMSDs, several ergonomic risk recognition approaches have  
156 been developed. For instance, observational-based approaches involve manual field observations  
157 and visual inspections of work-related risk factors and workers' activities by experienced expert  
158 observers. Examples of observational-based approaches used for recording and evaluating work-  
159 related risk factors include the Ovako Working Analysis System (OWAS) (Kivi and Mattila, 1991),  
160 the Rapid Upper Limb Assessment (RULA) (McAtamney and Corlett, 1993), and Rapid Entire  
161 Body Assessment (REBA) (Hignett and McAtamney, 2000). While OWAS is designed to  
162 recognize awkward postures in workers on manufacturing lines, the RULA tool evaluates  
163 ergonomic posture risks by calculating the angles between body parts. Zhang et al. (2018)  
164 performed ergonomic posture recognition from site cameras based on OWAS. Although  
165 observational-based approaches are applied to numerous work-related risk factors, they are mostly  
166 impractical due to the substantial cost, time, subjective judgments by the experts, and technical  
167 knowledge required for post-analysis of large amounts of non-heterogeneous data (David, 2005).

168

169 Vision-based approaches consist of the use of computer-aided visual sensing technologies, such  
170 as single or multi-video cameras, stereo cameras, depth cameras, and MS Kinect, to capture human  
171 motions and recognize WMSD risk factors in construction. Ray and Teizer (2012) utilized a depth  
172 camera to detect a worker's non-ergonomic postures by modeling the worker's skeleton and  
173 measuring its joint angles. Seo et al. (2015) proposed an approach that could perform 3D

174 biomechanical analysis using visionary data from a stereo camera. While vision-based approaches  
175 are intuitive and provide reliable results, they are limited to privacy and ethical issues since  
176 cameras are generally perceived as recording devices (Yilmaz et al., 2006). In addition, with the  
177 cluttered nature of the construction industry, characterized by diverse categories of specialized  
178 resources and risk factors, and continuously changing working conditions, they may result in  
179 several technical issues such as illumination and occlusion (Chen and Shen, 2017).

180  
181 In recent years, several researchers have utilized direct measurement approaches such as wearable  
182 sensor-based systems to recognize work-related risk factors for developing WMSDs among  
183 construction workers. Examples of these approaches include surface electromyography (sEMG),  
184 electrocardiography (ECG), photoplethysmography (PPG), electrodermal activity (EDA),  
185 electroencephalogram (EEG), WIMUs-based system, and wearable insole pressure system. Umer  
186 et al. (2017b) compared the differences in lumbar biomechanics (i.e., trunk muscle activity and  
187 trunk kinematics) during three typical rebar tying postures measured by sEMG and WIMUs.  
188 Similarly, Antwi-Afari et al. (2018a) investigated the risk of developing low back disorders in  
189 rebar workers by examining muscle activity and spinal kinematics during repetitive rebar lifting  
190 tasks by using sEMG and WIMUs. Yan et al. (2017) developed a real-time motion  
191 warning personal protective equipment that enables workers' self-awareness and self-management  
192 of ergonomically hazardous operational patterns for the prevention of WMSDs based on WIMUs.  
193 By using a wearable insole pressure system, Antwi-Afari and colleagues have proposed methods  
194 to recognize awkward working postures (Antwi-Afari et al., 2018f), and recognize overexertion-  
195 related workers' activities (Antwi-Afari et al., 2020a). While previous studies have made  
196 significant contributions for automated recognition of work-related risk factors for mitigating



197 WMSDs among construction workers, they mostly utilized direct measurement approaches in a  
198 laboratory experimental setting. In this regard, whether a wearable insole pressure system would  
199 perform well on a real construction dataset remains to be evaluated in this paper.

200

## 201 *2.2. Wearable sensor-based systems for automated recognition and WMSDs prevention*

202 Monitoring and recognizing workers' activities and work-related risk factors in real-time play a  
203 significant role in evaluating workers' productivity and mitigating WMSDs risks. Consequently,  
204 automated recognition of awkward working postures is an initial step for mitigating WMSDs. With  
205 recent advancements in information technologies, wearable sensor-based systems are mostly used  
206 as ergonomic intervention tools for proactive monitoring and recognizing workers' activities.  
207 Combined with computational analyses such as machine learning classifiers, these approaches  
208 have demonstrated their feasibility in the construction domain and provided good performance  
209 evaluation for recognizing workers' activities and work-related risk factors.

210

211 Numerous wearable sensor-based systems such as global positioning system (GPS), wearable  
212 biosensors (e.g., sEMG, ECG, PPG, EEG), ultra-wideband (UWB), and radio-frequency  
213 identification (RFID) are widely used for monitoring location-based activities, physiological  
214 responses, and detecting worker-object interactions (Antwi-Afari et al., 2019a). Caldas et al. (2006)  
215 assessed the potential of using GPS sensors to improve the tracking and location of materials on  
216 construction sites. Goodrum et al. (2006) developed a tool tracking and inventory system for  
217 storing operation and maintenance data by using commercially available active RFID tags. Xing  
218 et al. (2020) explored the effects of physical fatigue on the induction of mental fatigue in  
219 construction workers in a pilot experimental method by using wearable EEG sensors. Combining

220 the efforts of previous studies in the application of location tracking and proximity detection  
221 wearable sensor-based systems within the construction environment, they all provided reliable and  
222 more robust information for enhancing and monitoring construction operations such as workers,  
223 materials, and equipment. The main limitation for applying these location tracking and proximity  
224 detection wearable sensor-based systems is the need to install tags, sensors, or markers on each  
225 individual resource, which is costly and time-consuming and thereby makes deployment on  
226 construction sites unsuitable (Teizer et al., 2007).

227  
228 To overcome these challenges, researchers and practitioners have recently adopted WIMUs-based  
229 systems for human activity recognition and work-related risk factors recognition. WIMUs-based  
230 systems consist of an accelerometer, gyroscope, and magnetometer that measure 3-axes  
231 acceleration, angular velocity, and geomagnetic field, respectively. They are smaller in size, lighter  
232 in weight, have high capacity, and provide reliable accuracy for human activity recognition and  
233 WMSDs risk prevention. In the past decades, they have been widely used in research disciplines  
234 such as rehabilitation, sports science, and healthcare, to provide multimodal interactions, support  
235 independent living in elderly people, and context-aware personalized activity assistance  
236 (Mantjarvi et al., 2001; Bao and Intille, 2004; Delrobaei et al., 2018). Mantjarvi et al. (2001)  
237 recognize human ambulation and posture based on acceleration data collected from the hip.  
238 Delrobaei et al. (2018) proposed a WIMUs-based system to quantify full-body tremor and to  
239 separate tremor-dominant from non-tremor-dominant Parkinson's Disease patients and healthy  
240 individuals. In these previous studies, they suggested that WIMU-based systems could serve as a  
241 portable ergonomic intervention tool that can be used in the home environment to monitor patients  
242 and facilitate therapeutic interventions. In the realm of construction, numerous studies have also

243 focused on human activity recognition and WMSD prevention by using WMIUs-based systems  
244 (Joshua and Varghese, 2010; Valero et al., 2017; Alwasel et al., 2017; Chen et al., 2017). Despite  
245 significant efforts, attaching multiple WIMUs-based systems on workers' bodies lead to workers'  
246 discomfort and systemic instability, thus, limiting their application on construction sites.

247  
248 To remedy this situation and considering the rapid development of microelectromechanical  
249 systems (MEMS), WIMUs-based systems have become smaller to be incorporated into smart-  
250 wearable systems such as smartphones, smartwatches, smart belts, and smart wristbands for  
251 recognizing workers' activity and work-related risk factors. Smartphones and smart wearable  
252 systems are characterized as unobtrusive because they are embedded with multiple sensor-based  
253 systems (e.g., accelerometer, gyroscope, magnetometers, barometer, light and temperature  
254 sensors), which provide a self-sufficient data collection, computing, and storage scheme. In  
255 addition, they are more intelligent, intuitive, and ubiquitous wearable systems for wireless  
256 communication networks with modern software development environments and require relatively  
257 lower maintenance and operating cost as compared to WIMUs-based systems. These approaches  
258 have been widely applied in human activity recognition and work-related risk factors classification  
259 in construction (De Dominicis et al., 2013; Akhavian and Behzadan, 2016; Nath et al., 2018; Ryu  
260 et al., 2019). De Dominicis et al. (2013) investigated the capability of smartphones for real-time  
261 data collection of geo-localization information for construction site managers. Akhavian and  
262 Behzadan (2016) presented an activity analysis framework for recognizing and classifying various  
263 construction workers' activities by using a smartphone's built-in accelerometer and gyroscope  
264 sensors. Their method used five different types of machine learning algorithms to recognize  
265 various types of construction activities. The results indicate that neural networks outperform other

266 classifiers by offering an accuracy ranging from 87% to 97% for user-dependent and 62% to 96%  
267 for user-independent categories. Nath et al. (2018) proposed a method for monitoring ergonomic  
268 risk levels caused by overexertion through body-mounted smartphones (i.e., accelerometer, linear  
269 accelerometer, and gyroscope signals). By adopting a support vector machine (SVM) classifier,  
270 the results achieved an accuracy of 90.2%. Ryu et al. (2019) examined the feasibility of the wrist-  
271 worn accelerometer-embedded activity tracker for automated action recognition during simulated  
272 masonry work in a laboratory setting. It was found that the multiclass SVM with a 4-s window  
273 size showed the best accuracy (88.1%) for classifying four different subtasks of masonry work.  
274 These machine learning classifiers have been effectively demonstrated to recognize WMSD risk  
275 factors and workers' activities, but a remaining challenge is the lack of applicable features that  
276 accurately represent the change in a worker's bodily movements caused by awkward working  
277 postures. Nevertheless, smartphones with embedded sensor-based systems by their nature are not  
278 fixed wearable sensors because of varying device locations and orientations, which can lead to  
279 data misrepresentation.

280  
281 Given the above limitations, it is still crucial to deploy other automated wearable sensing systems  
282 for activity recognition and WMSDs prevention by collecting sensing data from workers on a  
283 construction site. In addition, it would be appropriate to select computational activity models that  
284 could allow software systems to conduct reasoning algorithms to infer workers' motion or  
285 movement. To do this, the current study seeks to evaluate a novel approach by using wearable  
286 insole sensor data and deep learning-based networks to automatically recognize and classify  
287 awkward working postures in construction. The next section provides more details on its feasibility  
288 and application on construction sites.

289        2.3. *Wearable insole sensor data and deep learning-based networks for recognizing*  
290            *awkward working postures in construction*

291 Automated recognition and classification of WMSD risk factors play a crucial role in mitigating  
292 WMSDs among construction workers. It could also help researchers and safety managers to  
293 retrieve important WMSD risk factor information to facilitate their analyses and decision-making  
294 support in WMSD prevention. Previous studies have extensively focused on the application of  
295 wearable insole sensor data and machine learning classifiers for recognizing and classifying loss  
296 of balance events (Antwi-Afari et al., 2018e), awkward working postures (Antwi-Afari et al.,  
297 2018f), and overexertion related construction activities (Antwi-Afari et al., 2020a). Antwi-Afari  
298 et al. (2018f) developed a non-invasive method to recognize and classify awkward working  
299 postures based on wearable insole pressure data and machine learning classifiers. The results  
300 achieved a classification accuracy of 99.7% by using the SVM, indicating the feasibility of using  
301 a wearable insole pressure system to recognize risk factors for developing WMSDs among  
302 construction workers. However, the main limitation of traditional machine learning classifiers is  
303 the fact that they treat individual dimensions of the sensor data statistically independently. Thus,  
304 each dimension of the data is converted into feature vectors without due consideration of their  
305 spatio-temporal context. To address this limitation, the current study adopted RNN-based deep  
306 learning models, which incorporate temporal dependencies of sensor data streams and are more  
307 appropriate for monitoring work-related risk factors than considering the data stream  
308 independently. Moreover, RNN-based deep learning models provide a high level of performance  
309 for time series sequential data classification, which serves as the memory units through the gradient  
310 descent steps.

311

312 Recently, deep learning networks have received great interest from the construction-related  
313 research fields because they have achieved exceptional performance in various research topics,  
314 including image classification (Yang et al., 2018; Zhong et al., 2020), object detection and  
315 recognition (Fang et al., 2018; Fang et al., 2018), natural language processing (Zhong et al., 2020),  
316 and work-related risk factors recognition (Zhang et al., 2018; Son et al., 2019; Yu et al., 2019; Kim  
317 and Cho, 2020; Lee et al., 2020; Yang et al., 2020; Zhao and Obonyo, 2020; Seo and Lee, 2021;  
318 Wang et al., 2021; Zhao and Obonyo, 2021). Son et al. (2019) presented a method to detect  
319 construction workers under varying poses against changing backgrounds in image sequences. Yu  
320 et al. (2019) analyzed a joint-level vision-based ergonomic assessment tool for construction  
321 workers (JVEC) to provide automatic and detailed ergonomic assessments of construction workers  
322 based on construction videos. The main limitation of vision-based ergonomic assessments (i.e.,  
323 images and videos) is that they require a direct line of sight to register the movements in a  
324 construction environment (Han and Lee, 2013).

325  
326 Kim and Cho (2020) achieved a classification performance of 82.39% to 94.73% accuracy for  
327 long-short term memory (LSTM) model than conventional machine learning classifiers. Lee et al.  
328 (2020) proposed an automatic detecting technique for excessive carrying-load (DeTECLoad) to  
329 predict load-carrying weights and postures, achieving 92.46% and 96.33% performance,  
330 respectively. Yang et al. (2020) adopted a bidirectional LSTM (Bi-LSTM) algorithm for physical  
331 load detection, and they achieved 74.6 to 98.6% accuracy. Zhao and Obonyo (2021) investigated  
332 the feasibility of deploying a convolutional long short-term memory (CLN) model under  
333 incremental learning for recognizing workers' posture and achieved 87% (personalized) and 84%  
334 (generalized) recognition performance. Wang et al. (2021) developed a novel vision-based real-

335 time monitoring, evaluation, and prediction method for workers' working postures. Their method  
336 achieved 87.0% accuracy of joint point recognition and 96.0% accuracy of posture risk prediction.  
337

338 The abovementioned previous studies applied various deep learning networks for recognizing and  
339 classifying work-related risk factors such as physical loads and awkward working postures.  
340 Compared to traditional machine learning classifiers, deep learning-based networks considerably  
341 reduce the effort of choosing the right features by automatically extracting abstract features  
342 through several hidden layers, and they have been proven to work well with unsupervised learning  
343 (Seyfioğlu et al., 2018; Nguyen et al., 2019) and reinforcement learning (Ijjina and Chalavadi,  
344 2017). The major limitation of these studies which hinders their application in construction is that  
345 wearable sensing data were collected by using WIMUs. It is known that attaching multiple  
346 WIMUs-based systems on workers' bodies lead to workers' discomfort and systemic instability,  
347 thus, limiting their application on construction sites (Antwi-Afari and Li, 2018g). Knowledge from  
348 these previous studies made significant contributions to automated work-related risk factors  
349 recognition for WMSD prevention, but still, there is a need to further improve the methods to  
350 prevent WMSDs in construction workers. Even though many previous studies on deep learning-  
351 based classification have been conducted, and the fact that human activity recognition, object  
352 detection and recognition, and WMSD risk recognition have widely been studied in construction,  
353 no recent study has utilized wearable insole sensor data collected from workers on construction  
354 sites as input data for recognizing and classifying awkward working postures among construction  
355 workers. To this end, the current study employs different types of deep learning networks to  
356 recognize and classify awkward working postures based on plantar pressure data collected from a  
357 wearable insole pressure system.

### 3. Research gaps, research objective, and contributions

Although awkward working postures remain one of the most prevalent work-related risk factors that may lead construction workers to develop WMSDs, little research has been conducted in recognizing and classifying different types of awkward working postures among construction workers. Thus, the main research question to be answered in this study is how to combine wearable insole sensor data and deep learning-based networks for recognizing and classifying different types of awkward working postures in construction. Given the above, the present study proposed a non-intrusive wearable insole sensor system for capturing plantar pressure data, and deep learning-based networks for awkward working posture recognition and classification. Therefore, the objective of this study was to recognize and classify different types of awkward working postures by using time-series wearable insole data and deep learning-based networks.

The main contributions of the present study can be summarized in two folds: (1) the feasibility of onsite experimental data collection for work-related risk factor recognition using a wearable insole pressure system. Numerous previous studies on work-related risk factor recognition are conducted by student participants in a controlled laboratory setting (Chen et al., 2017; Antwi-Afari et al., 2018f; Umer et al., 2020). These experimental conditions affect the generalization and validity of a given study. To improve the experimental design and data collection procedures, the present study analyzed wearable insole data collected from workers on construction sites for work-related risk factor recognition. Real time-series data collected from workers on construction sites are practically challenging due to the dynamic nature of the construction environment. Based on the field experiments, this study would provide a deeper insight towards validating the use of recognized awkward working postures performed by workers at the workplace; (2) occupational



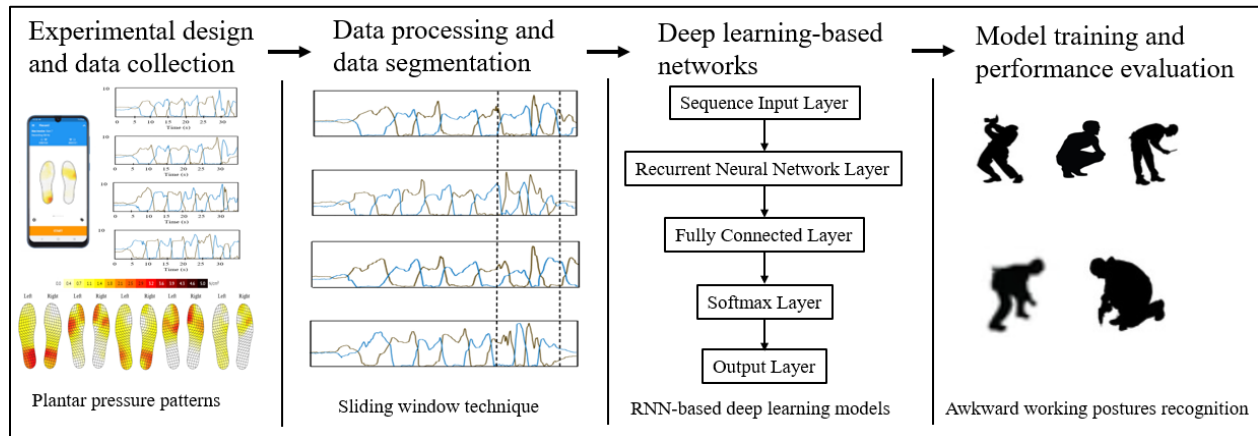
381 awkward working posture recognition and classification. In the construction domain, traditional  
382 ergonomics risk monitoring and recognition approaches (e.g., observational methods) for  
383 mitigating WMSDs are time-consuming, unreliable, and prone to errors. The proposed work-  
384 related risk factor recognition uses time-series wearable insole data (i.e., plantar pressure patterns)  
385 and RNN-based deep learning models (e.g., LSTM, Bi-LSTM, and gated recurrent units (GRU))  
386 for recognizing and classifying awkward working postures in construction. With this approach,  
387 workers' awkward working postures could be automatically monitored throughout the course of  
388 their work without any expert's interference or observation. In addition, this present study will add  
389 to the extant literature in this domain by utilizing both time series wearable insole sensor data and  
390 deep learning networks for practical application on construction sites. By adopting deep learning  
391 models, wearable insole data will be automatically extracted with highly representative features,  
392 containing spatio-temporal of plantar pressure patterns. Notably, this helps to enrich wearable  
393 sensor pattern data derived purely from time-series data for computational analysis and reasoning.  
394 Consequently, this proposed approach could enhance the generality and automation in construction  
395 safety management, especially for WMSD prevention.

396

#### 397 **4. Research methods**

398 This section discusses the experimental design and data collection procedures such as recruiting  
399 participants, experimental apparatus (i.e., wearable insole pressure system), and field experiment,  
400 and plantar pressure data collection from rebar workers on construction site. It also explains the  
401 data processing and data segmentation approach by adopting the sliding window technique. Next,  
402 three RNN-based deep learning models were adopted and discussed. The final stage is model  
403 training and performance evaluation, where each RNN-based deep learning model was trained by

404 using plantar pressure patterns as input data and the performance of the trained models was  
405 evaluated using metrics. Fig. 1 illustrates the framework of the proposed approach. Further details  
406 are presented below.



407  
408 **Fig. 1.** A framework of the proposed approach

409

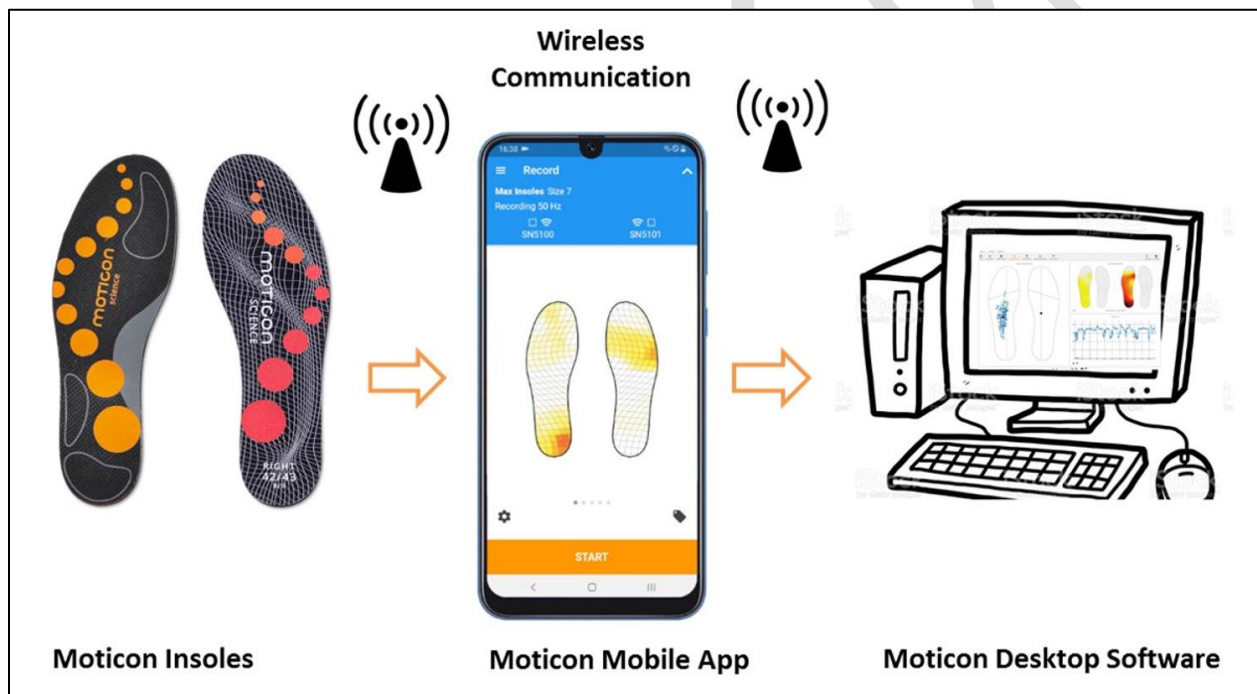
#### 410 4.1. *Experimental design and data collection*

##### 411 4.1.1. *Participants*

412 Ten male participants (i.e., construction rebar workers) were voluntarily recruited to participate in  
413 the experiments. Construction rebar workers were recruited and participated in this study because  
414 repetitive rebar tasks (e.g., preparing and assembling rebars) are physically demanding and often  
415 involve long working hours, awkward working postures, and manual lifting activities (Buchholz  
416 et al., 2003; Anwer et al., 2021). The participants mean age, weight, height, and shoe size were  $38$   
417  $\pm 1.82$  years,  $76 \pm 2.79$  kg,  $1.75 \pm 0.32$  m, and  $10.32 \pm 1.03$  EU size, respectively. All participants  
418 had no history of (1) significant foot injuries or lower extremity abnormalities during the last 12  
419 months preceding the start of the study, and (2) neurological conditions or disabilities or other  
420 conditions that affected fall and/or balance. The experimental protocol for data collection was  
421 reviewed and approved by the Institutional Review Board. In addition, a written consent was  
422 obtained from each participant after a verbal explanation of the experimental procedures.

423 4.1.2. *Experimental apparatus*

424 An OpenGo system (Moticon GmbH, Munich, Germany), which is a wearable insole pressure  
425 system for measuring plantar pressure distribution was used in the current study. Each left or right  
426 wearable sensor insole contains 16 capacitive pressure sensors, a 3-axis gyroscope (MEMS  
427 LSM6DSL, ST Microelectronics), and a 3-axis accelerometer. A sampling frequency of 50Hz was  
428 used for data collection. Further details of this wearable insole pressure system are presented in  
429 related studies (Antwi-Afari and Li, 2018g; Antwi-Afari et al., 2018e; Antwi-Afari et al., 2018f).  
430 Fig. 2 shows the overview of the mobile application user interface of the wearable insole system.



431 **Fig. 2.** Overview of the mobile application user interface of the wearable insole system  
432

433 4.1.3. *Field experiment and data collection*

435 Data collection was conducted on a construction site. Participants wore a safety boot with an  
436 inserted wearable insole. Each participant was studied during daily repetitive rebar tasks such as  
437 lifting, carrying, cutting, or tying rebars. While the participants performed their daily workplace  
438 activities, only five different types of awkward working postures were observed and collected.

439 They mainly included overhead working, squatting, stooping, semi-squatting, and one-legged  
440 kneeling. These awkward working postures were studied because they are often used in repetitive  
441 rebar tasks and expose rebar workers to high risk of developing WMSDs (Umer et al., 2017b;  
442 Antwi-Afari et al., 2018a). Fig. 3 depicts the field experimental trials of different types of awkward  
443 working postures. In the overhead working posture, participants were captured in an upright stance  
444 while working with their hands touching a bar above their head (Fig. 3a). Squat posture was  
445 identified when the participants maintained a full squat (Fig. 3b). Stoop posture involved full trunk  
446 flexion with bilateral knee extension in standing (Fig. 3c). Semi-squat posture involved bilateral  
447 knee bending (Fig. 3d). Lastly, one-legged kneeling was seen when the participants bent either of  
448 their knees to work in a kneeling position (Fig. 3e). Each participant performed a total of 75  
449 experimental tasks, consisting of 5 types of awkward working postures and 15 repeated  
450 experimental trials. Each experimental trial lasted for 30 seconds. Before field data collection, all  
451 participants were given sufficient time to familiarize themselves with the experimental apparatus  
452 (i.e., wearable insole pressure system) to eliminate systematic bias. The participants were also  
453 given enough rest (approx. 5 mins) between successive experimental trials to prevent injuries and  
454 physical fatigue. Notably, all experimental trials were conducted in an outdoor construction  
455 environment under natural conditions. The participants' plantar pressure data were synchronized  
456 and recorded by using a video camera for all experimental tasks. In this study, awkward working  
457 postures were defined as postures that deviated significantly from the neutral position and might  
458 cause WMSDs after being sustained for a long time (Karwowski, 2001). Moreover, it is worth  
459 mentioning that these awkward working postures exceeded the internationally recommended trunk  
460 inclination for the angles of various body parts for static working postures as defined by the  
461 International Organization for Standardization (ISO 11226:2000) (ISO, 2006).



(a) (b) (c) (d) (e)

462 **Fig. 3.** Field experiments of different types of awkward working postures: (a) Overhead working;  
 463 (b) Squatting; (c) Stooping; (d) Semi-squatting; and (e) One-legged kneeling  
 464

465

#### 466 *4.2. Data processing and data segmentation*

467 After data collection, the next stage is data processing and data segmentation. The collected data  
 468 were stored in the mobile phone, and they were wirelessly transferred onto a desktop computer for  
 469 data processing. For each observed awkward working posture, the participants performed 15  
 470 repeated trials. It is worth noting that the wearable insole pressure system can capture plantar  
 471 pressure patterns, acceleration, angular velocity, ground reaction force, and center of pressure data.  
 472 However, all the collected data except plantar pressure patterns data were removed from the dataset  
 473 during data processing. As such, only plantar pressure patterns were labelled and used for data  
 474 segmentation. Class labelling was conducted by using the recorded videos and the collected plantar  
 475 pressure data. The signals were visually inspected for noise or signal artefacts. Since plantar  
 476 pressure patterns were evenly distributed and didn't cause any unrelated changes to different types  
 477 of awkward working postures, no further signal artefacts were conducted during data processing.  
 478 In the data segmentation stage, a sliding window technique was adopted to divide plantar pressure  
 479 data into smaller segments, each segment containing a specified number of data samples (Preece  
 480 et al., 2009). The purpose of this stage is to obtain labeled segments from the continuous stream

481 of wearable insole data to evaluate the performance of the deep learning networks. Since the  
482 sampling frequency for data collection was 50 Hz, 50 data samples are obtained every second for  
483 data processing. Given the experimental conditions, the dataset contains 10 participants with  
484 1,125,000 data samples of five classes. By considering the conducted experiments which involved  
485 repetitive rebar tasks, a window size of 5.12 s, which represents 256 ( $2^8$ ) was suitable for dividing  
486 plantar pressure data into smaller segments. This window size data segment was chosen by initially  
487 analyzing the collected plantar pressure data to include representative awkward working postures  
488 in order to optimize the recognition performance. To prevent missing relevant data, an overlapping  
489 of consecutive windows was conducted. A 50% overlap of adjacent data segment lengths was used  
490 as demonstrated in previous studies (Antwi-Afari et al., 2018e; Antwi-Afari et al., 2018f).

491

#### 492 *4.3. Deep learning-based networks*

##### 493 *4.3.1. Recurrent neural network (RNN) model architectures*

494 RNN is a subset of deep learning-based networks on the principle of extracting the output layer  
495 and feeding it back as the input of another layer to predict the output of the current layer (Inoue et  
496 al., 2018). Fig. 4 represents an overview of the RNN model architecture. As shown in Fig. 4a, the  
497 basic architecture of an RNN consists of an input, output, activation function, and a recurrent loop.  
498 Fig. 4b illustrates the structure of an unfolded RNN into a full network that allows it to perform a  
499 sequence of input data. Generally, RNN model receives the input  $x_0$  from the sequence of input  
500 data, performs some calculations resulting in  $h_0$ , which, together with  $x_1$ , compose the input to the  
501 next step. Similarly, the output  $h_1$  with the input  $x_2$  will be the input to the next step, and so on. It  
502 is worth noting that  $y_t$  is the same as  $h_t$ .

503

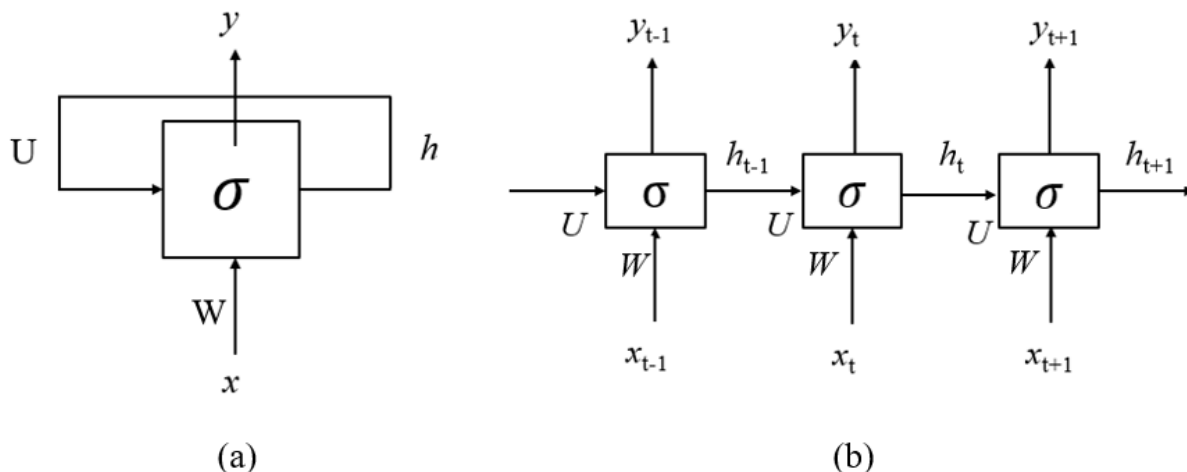
504 The value of  $h_t$  is calculated using Equation 1. As illustrated in Equation 1, the input  $x_t$  is modified  
 505 by  $W$  and  $h_{t-1}$  is modified by  $U$ .

$$506 \quad h_t = \sigma(Wx_t + Uh_{t-1}) \quad (1)$$

507 Where,  $x_t$  represents the input of the structure at time step  $t$ ,  $h_t$ , is the output of the structure at time  
 508 step  $t$ ,  $W$  is the weight matrix of the input to the hidden layer at time  $t$ ,  $U$  is the weight matrix of  
 509 the hidden layer at time  $t-1$ , and  $\sigma$  represents the activation function.

510

511 Like other neural network structures, RNN models learn weights ( $W, U$ ) through training using  
 512 the backpropagation technique. The network then determines the accuracy of the model by using  
 513 an error function (loss function) and calculating the derivatives of the loss function with respect to  
 514 the weight. In addition, the network uses an activation function to simplify the mathematical  
 515 calculations related to the application of backpropagation. In the following section, this study  
 516 presents three types of RNN-based deep learning models that were used for classifying different  
 517 types of awkward working postures.



518  
 519 **Fig. 4.** An overview of the RNN model architecture: (a) The basic architecture of an RNN; and (b)

520 The structure of an unfolded RNN

521 4.3.1.1. Long-short term memory (LSTM)

522 LSTM is a type of RNN model with an enhanced function to calculate hidden states. Hochreiter  
523 and Schmidhuber (1997) proposed LSTM network to solve temporal sequences and long-term  
524 dependency problems by adding the gating mechanism. Compared to traditional RNN models,  
525 LSTM network can solve the vanishing and exploding gradient problems because it extends RNN  
526 with memory cells which can ease the learning of temporal relationships on long time scales.

527

528 Fig. 5 shows LSTM cell architecture. This cell determines which data to keep in memory and  
529 which data to ignore using the concept of gating. LSTM cell has three gates, namely, input, forget,  
530 and output gates. These gates can be seen as write (deciding what new information should be kept  
531 in memory by the input gate), reset (deciding what information should be forgotten by the forget  
532 gate), and read (deciding what information should be output by the output gate) operations for the  
533 cells. LSTM cell state is the key component that carries the information between each LSTM cell.  
534 Modifications to the cell state are controlled by the three gates mentioned above. The first stage of  
535 the LSTM cell architecture is the forget gate, which is responsible for specifying which data to  
536 remember and which data to erase. This decision is made through the sigmoid layer as shown in  
537 Equation 2.

538 
$$f_t = \sigma(x_t W^f + h_{t-1} U^f + b_f) \quad (2)$$

539 The output is 0 or 1, where 0 means forget, and 1 means keep. The second stage is the input gate,  
540 which decides which information to be stored or added to the cell state. The input gate also consists  
541 of another sigmoid layer that is used to determine new candidate values that could be updated to  
542 the cell state, as shown in Equation 3.

543 
$$i_t = \sigma(x_t W^i + h_{t-1} U^i + b_i) \quad (3)$$



544 The next stage in LSTM is the memory update, where the old cell is updated to the new cell. The  
 545 *tanh* function creates a vector of candidate values that could be added to the state as shown in  
 546 Equation 4.

$$547 \quad \hat{C}_t = \tanh(x_t W^g + h_{t-1} U^g + b_c) \quad (4)$$

548 The cell state is then ready for the update by concatenating both  $f_t$  and  $\hat{C}_t$ . LSTM updates the old  
 549 cell state  $C_{t-1}$  to be  $C_t$  as shown in Equation 5.

$$550 \quad C_t = \sigma(f_t \times C_{t-1} + i_t \times \hat{C}_t) \quad (5)$$

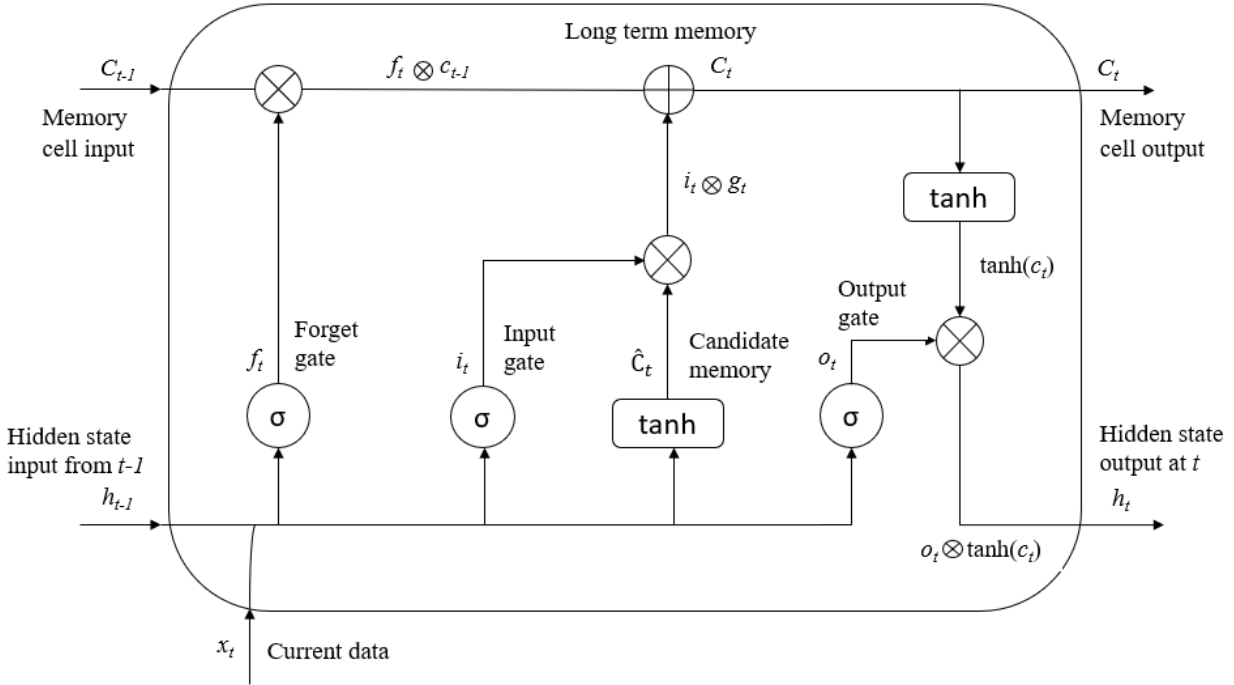
551 The final stage of LSTM is the *output gate*, which uses a sigmoid function to determine which part  
 552 of the cell state will come out as shown in Equation 6.

$$553 \quad o_t = \sigma(x_t W^o + h_{t-1} U^o + b_o) \quad (6)$$

554 In Equation 7, by multiplying  $o_t$  with  $\tanh(C_t)$ , we implicitly determine which part to take out.

$$555 \quad h_t = \tanh(C_t) \times o_t \quad (7)$$

556 Where,  $i_t$ ,  $f_t$ , and  $o_t$  are the input, forget, and output gates, respectively.  $W^i$ ,  $W^f$ , and  $W^o$  are the  
 557 weights for the input, forget, and output gates at time step  $t$ , respectively.  $W^g$  is the weight for the  
 558 candidate layer.  $U^i$ ,  $U^f$ , and  $U^o$  are the weights for the input, forget, and output gates at time step  
 559  $t-1$ .  $U^g$  is the weight for the candidate layer.  $x_t$  is the input at current time step  $t$ .  $h_t$  and  $h_{t-1}$  are the  
 560 output of the cell at current time step  $t$  and previous time step  $t-1$ , respectively.  $C_t$  and  $C_{t-1}$  are the  
 561 cell states at time steps  $t$  and  $t-1$ , respectively.  $b_i$ ,  $b_f$ , and  $b_o$  are the biases for the input, forget, and  
 562 output gates, respectively.  $b_c$  is the bias for the candidate layer, and  $\sigma$  is the sigmoid function.



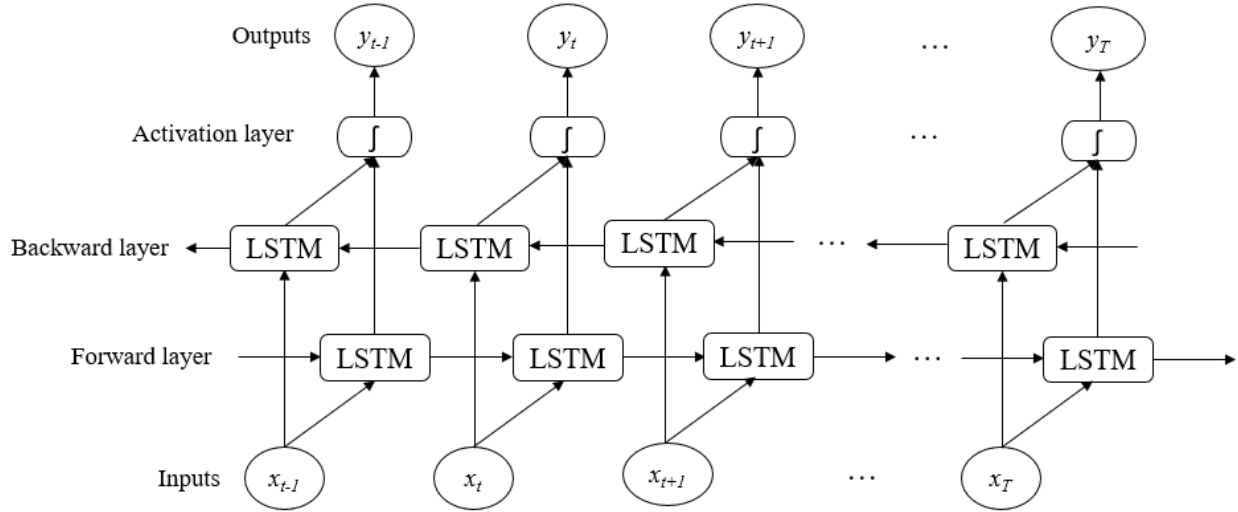
563  
564 **Fig. 5.** LSTM cell architecture

565

566 *4.3.1.2. Bidirectional LSTM (Bi-LSTM)*

567 Fig. 6 depicts the Bi-LSTM layer structure, where the two independent layers share the same input  
 568 sequence while the outputs from the two layers are concatenated and represented in the sequence.  
 569 Bi-LSTM model consists of two separate layers that divide the state neurons of a regular LSTM  
 570 into a forward layer, which is responsible for positive time direction, and a backward layer, which  
 571 is responsible for negative time direction. The outputs of the forward and backward layers are  
 572 concatenated, which make it possible to obtain the forward and backward information at each time  
 573 step in the sequence. This approach enhances the learning process due to the dependency found  
 574 between the neighboring data pairs.

575



576  
577 **Fig. 6.** Bi-LSTM layer structure

578

#### 579 4.3.1.3. Gated recurrent units (GRU)

580 GRU is an improved version of the standard RNN and a simplified version of LSTM (Gers et al.  
581 2002). Like LSTM, GRU is designed to reset or update its memory adaptively. Hence, GRU has a  
582 reset gate and an update gate, which are identical to the forget and the input gates in LSTM. Fig.  
583 7 represents the GRU cell architecture, which is like the LSTM structure but with fewer parameters  
584 that enable it to capture long-term dependencies more easily. The update gate monitors the amount  
585 of memory content that must be forgotten from the previous time step.

586 The operation of a GRU cell can be described as follows:

$$587 \quad z_t = \sigma(W_z \cdot [h_{t-1}, x_t] + b_z) \quad (8)$$

588 The model uses the reset gate to decide the amount of past information to forget as given in  
589 Equation 9.

$$590 \quad r_t = \sigma(W_r \cdot [h_{t-1}, x_t] + b_r) \quad (9)$$

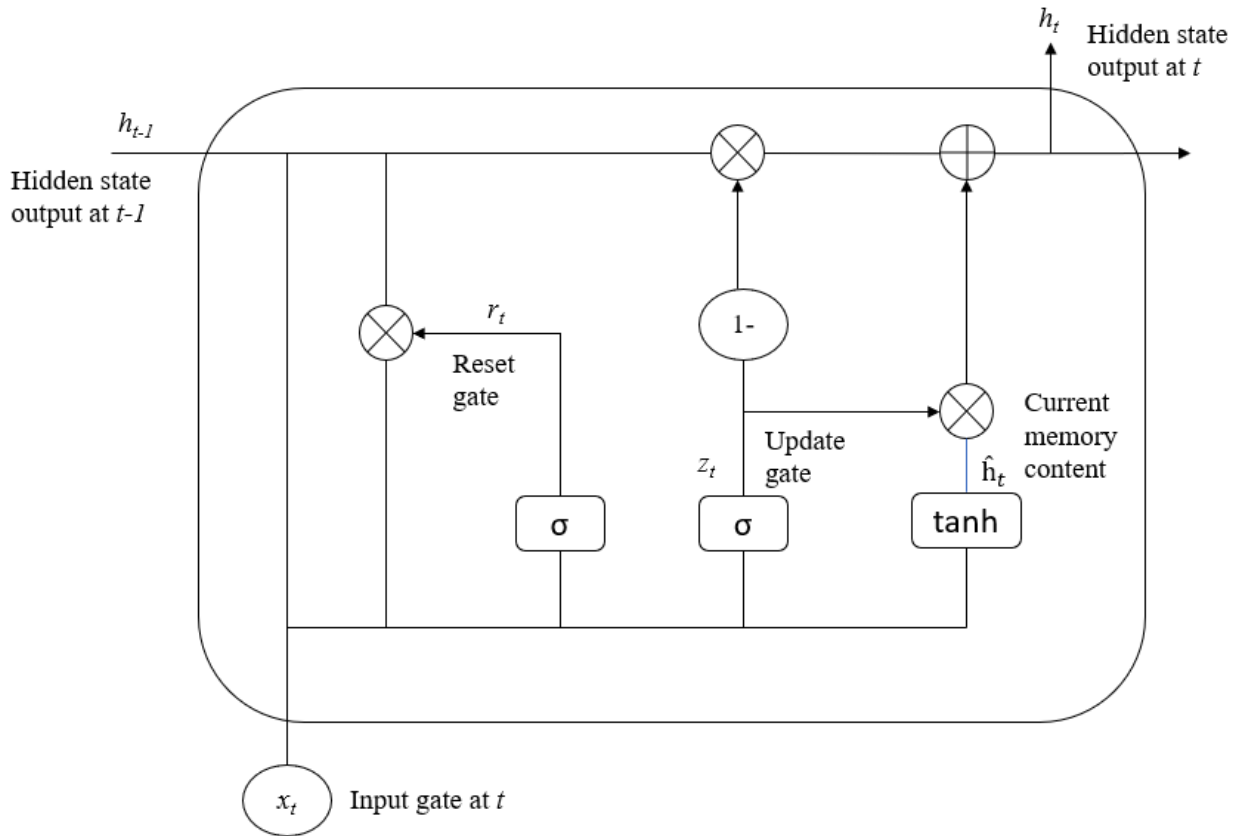
591 New memory content is introduced by using the reset gate as calculated in Equation 9 and relevant  
592 past information is stored as shown in Equation 10.

593 
$$\hat{h}_t = \tanh(W \cdot [r_t \times h_{t-1}, x_t] + b_h) \tag{10}$$

594 Finally, the network calculates the hidden state  $h_t$ , which is a vector that carries information for  
 595 the current unit and passes it down to the network. Thus, the update gate is essential since it decides  
 596 what is needed from the current memory content  $\hat{h}_t$  and the previous step  $h_{t-1}$ . Equation 11  
 597 calculates the value of  $h_t$ .

598 
$$h_t = (1 - z_t) \times h_{t-1} + z_t \times \hat{h}_t \tag{11}$$

599 Where,  $z_t$  and  $r_t$  are the output of the update and reset gates.  $W_z$  and  $W_r$  are the weights for the  
 600 update and reset gates.  $b_z$  and  $b_r$  are the biases for the update and reset gates.  $h_t$  and  $h_{t-1}$  are the  
 601 output of the cell at the current time step  $t$  and previous time step  $t-1$ , respectively.  $x_t$  is the input  
 602 at the current time step  $t$ , and  $\sigma$  is the sigmoid function.



603  
 604 **Fig. 7.** GRU cell architecture

#### 605 4.4. *Deep learning model training and performance evaluation*

606 During the deep learning model training, all RNN-based deep learning models (i.e., LSTM, Bi-  
607 LSTM, and GRU) have been designed to receive the same input data. Each class label belongs to  
608 the same participant from plantar pressure data. For each experimental task, the plantar pressure  
609 data vector has a dimensionality of 32 vectors ( $2 \times 16$  pressure sensors for each foot)  $\times$  256 data  
610 samples. The total number of data samples is 4,394 values. Since each window size contains 256  
611 data samples, the current study used input data of 1,124,864 data samples. The network models  
612 are three layers deep, and the number of hidden units ranges from 100 to 500 for each deep learning  
613 model. A previous study used a similar architecture, with 200 hidden units per layer (Alawneh et  
614 al., 2021). In this study, we used the cross-entropy loss (log loss function) as a cost function for  
615 model accuracy. The loss function determines the model's accuracy in the classification problem.  
616 The smaller the loss value, the more accurate the actual value. Updating the weights and biases in  
617 the model is the responsibility of the optimization function. In addition to the Adam optimization  
618 function, an adaptive version of the stochastic gradient descent was used for model training  
619 (Kingma and Ba, 2014). The Adam optimizer is a reliable optimizer that ensures fast and accurate  
620 results when updating the network parameters. To prevent overfitting in the model, this study  
621 applied the widely used stochastic regularization method known as the dropout technique  
622 (Srivastava et al., 2014). Overfitting arises when the loss function is very small for training data  
623 while it is very large for testing data. The main objective of the dropout technique is to prevent the  
624 neurons in the network from excessive co-adapting, which results in a lack of model generalization.  
625 The model evaluation process is performed by dividing the dataset into training and testing datasets,  
626 thus, 90% for training and the remaining 10% for testing. The training dataset was further split  
627 into two datasets (80% for training and 20% for validation). The validation dataset was used for

628 hyper-parameter tuning and to determine the optimal unit numbers of the RNN-based deep  
629 learning models. The 10-folds cross-validation technique was adopted to test the classification  
630 performance of RNN-based deep learning models, similar to previous studies utilizing deep  
631 learning networks (Kim and Cho, 2020; Yang et al., 2020). By conducting 10-folds cross-  
632 validation, the best hyper-parameters can be selected, and the RNN-based deep learning models  
633 can be evaluated as generalized models that show the desired classification performance with an  
634 unseen dataset. The parameters values based on the model that provided the best accuracy with the  
635 lowest training time were selected. The results show that our tuning process achieved the best  
636 accuracy for the datasets when setting the values of the epoch, dropout, batch size, learning rate,  
637 and hidden units at 100, 0.5, 64, 0.001, and 200, respectively. The experiments were conducted  
638 and trained on a computer 2.60 GHz Intel (R) Core (TM) i7-9750H CPU, 16GB RAM, 64-bit  
639 operating system, Windows 10 Pro, and Intel Iris Plus Graphics 650 1536MB GPU using  
640 MATLAB R2020b. The detailed dataset and tuned hyper-parameters of the proposed RNN-based  
641 deep learning models are shown in Table 1.

642 **Table 1.** Dataset and hyper-parameters of the proposed RNN-based deep learning models

<b>Dataset and hyper-parameters</b>	<b>Value</b>
Number of classes	5
Number of plantar pressure sensors	32 capacitive pressure sensors
Window size	5.12 s
Overlap of adjacent windows	50%
Sampling rate	50 Hz
Epoch	100
Dropout	0.5
Batch size	64
Learning rate	0.001
Hidden units	200
Number of sample data	1,125,000 data samples

643  
644 In performance evaluation and classification, the performance of the three types of RNN-based  
645 deep learning models was assessed by using evaluation metrics such as accuracy, precision, recall,

646 specificity, and F1-score (Attal et al. 2015). Equations 12 to 16 show how each evaluation metric  
647 is calculated. Accuracy is the most standard metric to summarize the overall classification  
648 performance for all classes. It is defined as the ratio of correctly classified instances to the total  
649 number of instances. Precision is the measure of determining how many instances classified as  
650 positive are actually positive, thus, it is a measure of exactness. It is defined as the ratio of correctly  
651 classified positive instances to the total number of instances classified as positive. Recall or  
652 sensitivity is the number of positive instances correctly classified as positive, thus, it is a measure  
653 of correctness. It is defined as the ratio of correctly classified positive instances to the total number  
654 of positive instances. Specificity is the number of negative instances correctly classified as  
655 negative. It is defined as the ratio of correctly classified negative instances to the total number of  
656 instances classified as negative. The F1-score combines precision and recall into a single value,  
657 and it is used to measure the performance of the classification model by avoiding systematic bias  
658 (Ordóñez and Roggen, 2016). Besides these evaluation metrics, the performance of each model on  
659 individual classes was assessed using a confusion matrix, while the accuracy and loss curves were  
660 drawn for the best model.

$$661 \text{ Accuracy} = \frac{TP + TN}{TP + TN + FP + FN} \quad (12)$$

$$662 \text{ Precision} = \frac{TP}{TP + FP} \quad (13)$$

$$663 \text{ Recall} = \frac{TP}{TP + FN} \quad (14)$$

$$664 \text{ Specificity} = \frac{TN}{TN + FP} \quad (15)$$

$$665 \text{ F1 - score} = 2 \times \frac{\text{Precision} \times \text{Recall}}{\text{Precision} + \text{Recall}} \quad (16)$$

666 Where, True Positive (TP) is the number of positive instances that were classified as positive, True  
667 Negative (TN) is the number of negative instances that were classified as negative, False Positive  
668 (FP) is the number of negative instances that were classified as positive, and False Negatives (FN)  
669 is the number of positive instances that were classified as negative.

670

## 671 5. Results

672 This section presents the results derived from the conducted experimental design and data  
673 collection procedures. Table 2 shows the classification accuracy and training time for different  
674 types of RNN-based deep learning models which were evaluated by 10-folds cross-validation. The  
675 classification accuracy for all three RNN-based deep learning models was greater than 97%. As  
676 indicated in Table 2, the classification accuracies were 97.99%, 98.33%, and 99.01% for LSTM,  
677 Bi-LSTM, and GRU, respectively. The results revealed that GRU model achieved the highest  
678 performance among all tested RNN-based deep learning models in terms of training plantar  
679 pressure pattern data for classifying different types of awkward working postures. On the other  
680 hand, when the performance of the three types of RNN-based deep learning models was evaluated  
681 in terms of training time, the average duration of LSTM, Bi-LSTM, and GRU networks lasted 31  
682 mins, 56 mins, and 54 mins, respectively. The results show that Bi-LSTM network requires more  
683 training time than either LSTM or GRU models.

684 **Table 2.** Classification accuracy and training time for RNN-based deep learning models

RNN-based deep learning models	Accuracy (%)	Training time (minutes)
Long-short term memory (LSTM)	97.99	31
Bidirectional LSTM (Bi-LSTM)	98.33	56
Gated recurrent units (GRU)	99.01	54

685

686 The confusion matrix and evaluation metrics for LSTM model are presented in Table 3. Generally,  
687 the evaluation metrics achieved high performance of LSTM model on the plantar pressure data for



688 classifying different types of awkward working postures. In terms of precision metric, LSTM  
689 model achieved classification performance values between 88.30% and 99.82%. The highest  
690 instance of correct classified awkward working posture was overhead working posture,  
691 representing 98.74%. Conversely, stooping posture had little impact on the LSTM model (i.e.,  
692 67.48%) among the different types of awkward working postures. The values of specificity and  
693 F1-score metrics are in the range of 95.33% to 99.94%, and 76.50% to 98.40%, respectively. To  
694 identify the classes that are misclassified or confused with other classes, the confusion matrix was  
695 presented. As shown in Table 3, each row represents the actual classes, while the columns represent  
696 the predicted classes. The diagonal cells represent the correct instances as highlighted in bold font  
697 for a more detailed evaluation of the classification performance at the end of the 100<sup>th</sup> epoch. The  
698 other cells show the misclassified instances. From Table 3, it was revealed that overhead working  
699 posture class had the best recognition performance because plantar pressure data are different from  
700 the values in other classes. It can also be seen that the top two most misclassified classes are  
701 stooping and overhead working postures. Stooping posture is confused 30 times with overhead  
702 working posture. Data collection for both stooping and overhead working postures involved  
703 bilateral knee extension in static positions. As such, the confusion between stooping and overhead  
704 working postures can be explained by the similar plantar pressure data collected from the wearable  
705 insole system.

706 **Table 3.** Confusion matrix and evaluation metrics for long-short term memory (LSTM)

		<b>Predicted class</b>				
<b>True class</b>	Overhead working	<b>625</b>	0	5	3	0
	Squatting	10	<b>350</b>	4	3	1
	Stooping	30	4	<b>83</b>	6	0
	Semi-squatting	23	0	2	<b>433</b>	0
	One-legged kneeling	8	0	0	9	<b>533</b>
		Overhead working	Squatting	Stooping	Semi-squatting	One-legged kneeling
<b>Accuracy</b>						97.99%
<b>Precision</b>		89.80%	98.87%	88.30%	95.37%	99.82%
<b>Recall</b>		98.74%	95.11%	67.48%	94.54%	97.02%
<b>Specificity</b>		95.33%	99.78%	99.46%	98.76%	99.94%
<b>F1-score</b>		94.06%	96.95%	76.50%	94.96%	98.40%

707

708 Table 4 represents the confusion matrix and evaluation metrics of Bi-LSTM model. The correct  
709 classes are shown in bold for a more detailed evaluation of the classification performance at the  
710 end of the 100<sup>th</sup> epoch. Generally, the evaluation metrics of Bi-LSTM model achieved higher  
711 performance than LSTM model. With regards to precision metric, Bi-LSTM model achieved  
712 performance rates between 92.09% and 99.61%. Like LSTM model, the highest instance of Bi-  
713 LSTM for correct classified awkward working posture was overhead working, representing  
714 97.83%. It was reported that overhead working posture had the most positive impact on the  
715 performance of Bi-LSTM, followed by one-legged kneeling (97.80%), squatting (96.37%), semi-  
716 squatting (93.02%), and stooping (87.50%) (Table 4). The specificity and F1-score metrics of  
717 different types of awkward working postures range from 96.03% to 99.88% and 91.70% to 98.75%,  
718 respectively. According to the confusion matrix in Table 4, it can be observed that overhead  
719 working posture is the most recognized class with 675 positive instances. In addition, it was found  
720 that the top two most misclassified classes are stooping and overhead working postures (Table 4).

721

722 **Table 4.** Confusion matrix and evaluation metrics for bidirectional LSTM (Bi-LSTM)

		Predicted class				
<b>True class</b>	Overhead working	<b>675</b>	0	8	5	2
	Squatting	8	<b>425</b>	0	8	0
	Stooping	25	2	<b>210</b>	3	0
	Semi-squatting	18	0	0	<b>240</b>	0
	One-legged kneeling	7	0	0	4	<b>512</b>
		Overhead working	Squatting	Stooping	Semi-squatting	One-legged kneeling
<b>Accuracy</b>					98.33%	
<b>Precision</b>	92.09%	99.53%	96.33%	92.31%	99.61%	
<b>Recall</b>	97.83%	96.37%	87.50%	93.02%	97.80%	
<b>Specificity</b>	96.03%	99.88%	99.58%	98.94%	99.88%	
<b>F1-score</b>	94.87%	97.93%	91.70%	92.66%	98.75%	

723

724 The confusion matrix and evaluation metrics of GRU model are presented in Table 5 with correct

725 classes shown in bold for a more detailed evaluation of the classification performance at the end

726 of the 100<sup>th</sup> epoch. The evaluation metrics of GRU model achieved the highest performance

727 compared to either LSTM or Bi-LSTM model. Regarding precision metric, GRU model achieved

728 classification performance values between 94.41% and 99.80%. The highest instance of correct

729 classified awkward working posture was overhead working, representing 99.30%. This recall

730 result concurs with classification accuracy, thus, indicating that GRU model outperforms other

731 RNN-based deep learning models. It was found that stooping posture had the lowest correct

732 classified posture (i.e., 89.00%) among the different types of awkward working postures. The

733 specificity and F1-score metrics of different types of awkward working postures range from 97.08%

734 to 99.94% and 93.19% to 99.39%, respectively. Taken together, these results show that GRU

735 model outperformed either LSTM or Bi-LSTM model based on plantar pressure data for

736 classifying different types of awkward working postures. Like LSTM and Bi-LSTM models, it can

737 be observed from the confusion matrix in Table 5 that overhead working posture is the most

738 recognized class with 710 positive instances. Moreover, it was reported that stooping and overhead  
 739 working postures are the top two most misclassified classes (Table 5).

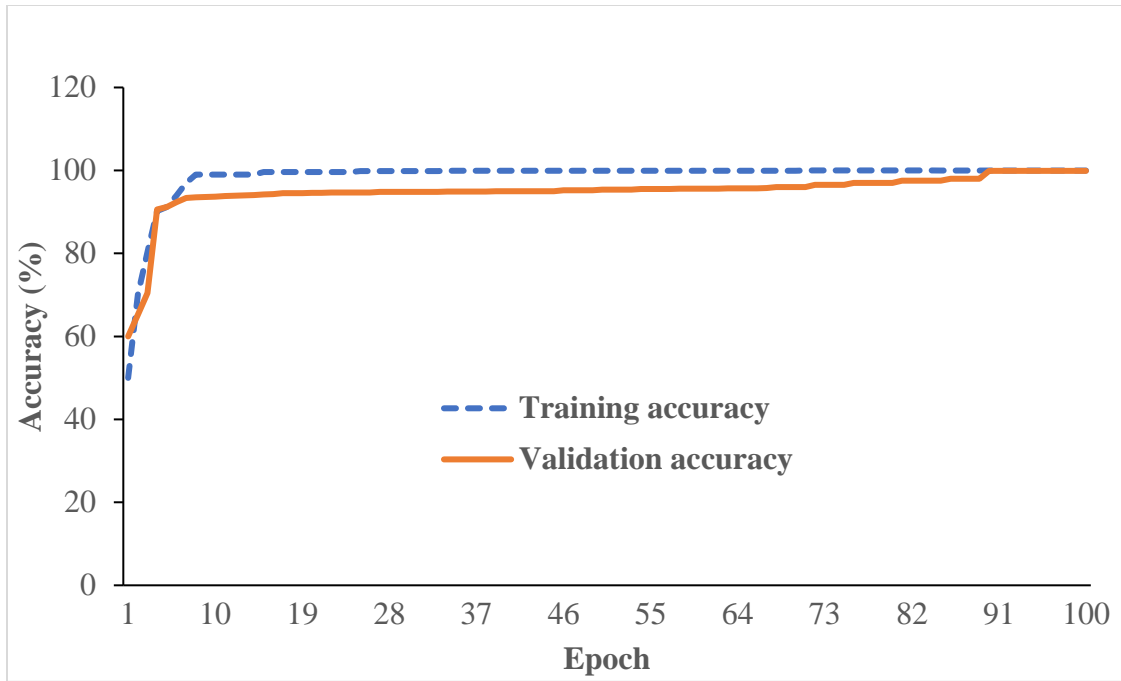
740

741 **Table 5.** Confusion matrix and evaluation metrics for gated recurrent units (GRU)

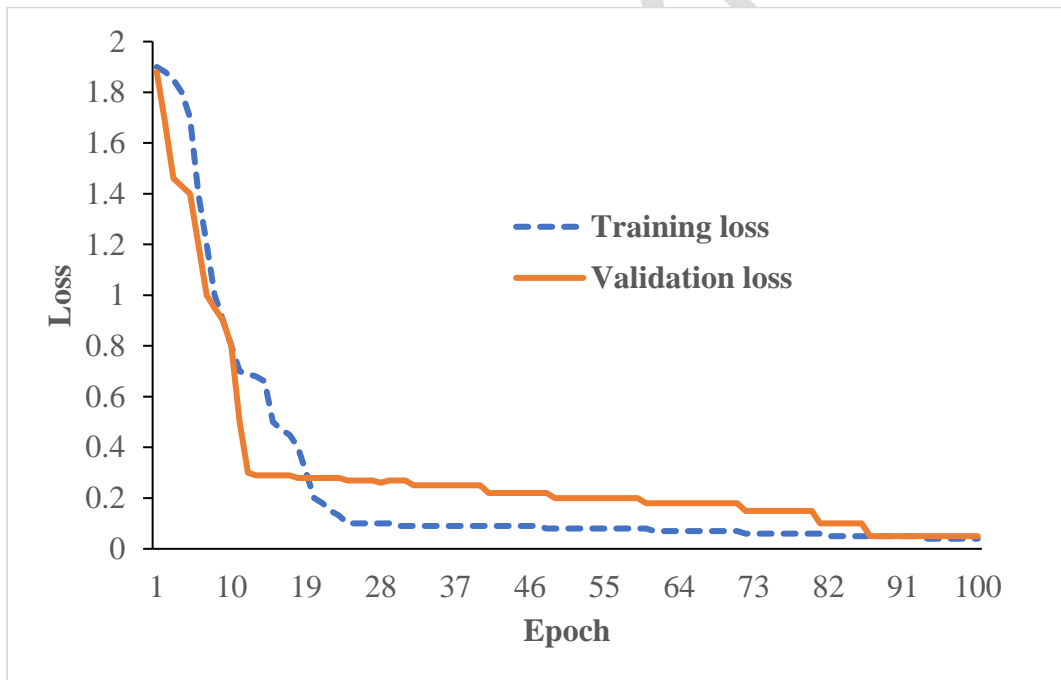
		<b>Predicted class</b>				
<b>True class</b>	Overhead working	<b>710</b>	0	4	1	0
	Squatting	5	<b>412</b>	0	3	0
	Stooping	21	1	<b>178</b>	0	0
	Semi-squatting	12	0	0	<b>310</b>	1
	One-legged kneeling	4	0	0	1	<b>489</b>
		Overhead working	Squatting	Stooping	Semi-squatting	One-legged kneeling
<b>Accuracy</b>						99.01%
<b>Precision</b>		94.41%	99.76%	97.80%	98.41%	99.80%
<b>Recall</b>		99.30%	98.10%	89.00%	95.98%	98.99%
<b>Specificity</b>		97.08%	99.94%	99.80%	99.73%	99.94%
<b>F1-score</b>		96.80%	98.92%	93.19%	97.18%	99.39%

742

743 Fig. 8 and 9 show the accuracies and losses over iterations curves with the tuned hyperparameters  
 744 of the GRU model. As shown in both figures, GRU model performance shows an increase in  
 745 accuracy and decrease in loss in both training and validation, respectively. In other words, the  
 746 training and validation curves for GRU model converge at higher accuracy whilst their  
 747 corresponding loss curves converge at a lower loss value. It was found that both the accuracies and  
 748 losses were converged at the 90<sup>th</sup> epoch. Thus, the difference between either training accuracy and  
 749 validation accuracy or training loss and validation loss was insignificant, indicating that the GRU  
 750 model was effectively trained without overfitting plantar pressure data.



751  
 752 **Fig. 8.** Accuracies over iterations curves with the tuned hyperparameters of the GRU model  
 753



754  
 755 **Fig. 9.** Losses over iterations curves with the tuned hyperparameters of the GRU model  
 756

757 6. **Discussion**

758 *6.1. Wearable sensing data and deep learning-based networks*

759 Construction activities are associated with several work-related risk factors. Among them,  
760 awkward working postures are the major risk factor that causes WMSDs in construction. The  
761 objective of this research was to evaluate a novel approach of using deep learning-based networks  
762 and wearable insole sensor data to automatically recognize and classify different types of awkward  
763 working postures in construction. To do this, this study adopted three types of RNN-based deep  
764 learning models to train time-series plantar pressure data captured by a wearable insole system.

765  
766 By comparing the employed RNN-based deep learning models in this study, it was found that  
767 GRU model achieved the highest accuracy (i.e., 99.01%) with an average training duration of 54  
768 minutes. In addition, the results show that GRU model obtained precision, recall, specificity, and  
769 F1-score metrics of 94.41% to 99.80%, 89.00% to 99.30%, 97.08% to 99.94%, and 93.19% to  
770 99.39%, respectively in classifying different types of awkward working postures. Regarding the  
771 confusion matrix, it was revealed that the top two most misclassified classes are stooping and  
772 overhead working postures. Moreover, GRU model performance shows an increase in accuracy  
773 and a decrease in loss in both training and validation, respectively. These results support the  
774 hypothesis of this study that GRU model, which is an RNN-based deep learning network could  
775 provide a reliable and better performance accuracy for classifying different types of awkward  
776 working postures. This finding might be explained from the model perspective. GRU model is  
777 relatively simpler and can forget and choose memory with fewer parameters, while LSTM model  
778 needs more gating and parameters to complete similar tasks. In addition, GRU model can control  
779 the information flow from the previous activation when computing new candidate activation. In

780 summary, GRU model outperformed other RNN-based deep learning models in this study in terms  
781 of computational power (i.e., convergence of training time) and performance (i.e., parameter  
782 updates). Our results are comparable to other previous studies which found GRU model to  
783 outperform LSTM model (Yang et al., 2020; Zarzycki and Ławryńczuk, 2021). The findings of  
784 this study indicate that GRU architecture can leverage the advantages of both LSTM and Bi-LSTM  
785 layer architectures to enhance awkward posture recognition. Hence, the use of the GRU model is  
786 recommended for classifying awkward working postures based on wearable insole data.

787  
788 A previous study by Antwi-Afari et al. (2018f) utilized plantar pressure data to recognize different  
789 types of awkward working postures based on machine learning classifiers, finding an accuracy of  
790 99.70% with SVM classifier at 0.32s window size. However, this previous work was conducted in  
791 a controlled laboratory setting, by student participants, and static awkward working postures.  
792 These experimental conditions are not the case in a real-world construction environment. By  
793 utilizing WIMU-based systems, Lee et al. (2020) compared a deep learning network (i.e., CNN-  
794 LSTM) to conventional machine learning classifiers for automated classification of squat postures.  
795 They obtained 75.4% and 91.7% classification performance for conventional machine learning  
796 and deep learning model, respectively. Although these results are comparable to the current study,  
797 Lee et al. (2020) used acceleration and angular velocity data while the present study used plantar  
798 pressure data captured by a wearable insole system.

799  
800 Notably, previous studies have also demonstrated similar deep learning networks (e.g., vanilla,  
801 unidirectional LSTM, Bi-LSTM, GRU) in wearable sensor-based human activity recognition  
802 studies in construction (Rashid and Louis, 2019; Kim and Cho, 2020; Lee et al., 2020; Yang et al.,

2020; Zhao and Obonyo, 2021) and other disciplines (Li et al., 2019; Alawneh et al., 2021; Mekuksavanich and Jitpattanakul, 2021). Rashid and Louis (2019) evaluated a data-augmentation framework for identifying construction equipment activity by combining LSTM model and multiple WIMU-based systems. They found that LSTM model outperforms conventional machine learning classifier (i.e., artificial neural network). Kim and Cho (2020) proposed a construction worker's motion recognition model using the LSTM network based on an evaluation of the number and location of WIMUs to maximize motion recognition performance. They found that the proposed approach could improve a worker monitoring mechanism for safety and productive management. Yang et al. (2020) investigated the feasibility of identifying various physical loading conditions by analyzing a worker's bodily movements collected by using WIMUs. Their findings contribute to automated work-related risk recognition and WMSDs prevention, thus, enhancing workers' health and safety at construction workplace. Zhao and Obonyo (2020) investigated the feasibility of integrating convolutional neural networks (CNN) with LSTM layers for recognizing construction workers' postures from motion captured by WIMUs-based systems. The results revealed that the proposed deep neural network approach has a high potential in addressing challenges for improving posture recognition performance than conventional machine learning models. Alawneh et al. (2021) compared the performance of data augmentation and RNN-based deep learning models on three open-source datasets, finding that GRU models and data augmentation significantly enhance activity recognition. Collectively, these studies found that deep learning models and wearable sensing data can be utilized for monitoring workers' activities regarding their safety, fall risks, and productivity. However, direct comparison between existing studies' findings and the current study may not be meaningful due to numerous differences in experimental design (e.g., participants' physical characteristics) and data collection procedures.



826 *6.2. Study implications, practical applications, and contributions*

827 The current study provides relevant findings and practical implications to both researchers and  
828 practitioners within the construction industry. First, a key practical implication is the feasibility of  
829 onsite experimental data collection for work-related risk factor recognition using a wearable insole  
830 pressure system. Collecting wearable sensing data in a real-world construction setting is very  
831 challenging due to multiple reasons such as the dynamic nature of the construction environment,  
832 huge resources, and several work-related risk factors. Different from previous studies on work-  
833 related risk factor recognition that were conducted by student participants in a controlled  
834 laboratory setting (Chen et al., 2017; Antwi-Afari et al., 2018f; Umer et al., 2020), the current  
835 study investigated the use of wearable insole data while construction rebar workers performed  
836 awkward working postures during repetitive rebar tasks at construction site. Awkward working  
837 postures are also commonly performed by other workers such as masons, carpenters in the  
838 construction industry. Collectively, the proposed approach could not only be applied during  
839 repetitive rebar tasks (e.g., preparing and assembling rebars), but also other manual repetitive  
840 handling tasks (e.g., bricklaying) in construction. Second, the proposed approach provides an  
841 automated recognition and classification of awkward working postures in construction. The results  
842 from the current study revealed that awkward working postures, the most prevalent work-related  
843 risk factor among construction workers, could be recognized and classified by using wearable  
844 insole data and deep learning networks. Awkward posture recognition is the first step in proactive  
845 WMSD prevention. As such, this wearable sensor-based approach can serve as a proactive  
846 intervention tool for recognizing work-related risk factors, thus, mitigating WMSDs risks in  
847 construction. Besides automated WMSDs risk monitoring and recognition in construction, the  
848 achieved awkward posture recognition model can also facilitate “Prevention through Design” (PtD)

849 practices by identifying workers' ergonomic risks under different workplace designs. These  
850 preventive strategies can also be adopted in other physically demanding and labor-intensive  
851 occupations such as manufacturing, automobile, and agriculture. Third, the proposed approach—  
852 utilizing wearable insole data and deep learning-based networks—will contribute to real-time  
853 wearable sensor computing by deploying the performance of plantar pressure patterns and GRU  
854 model for awkward posture recognition. Construction practitioners (e.g., safety managers) can use  
855 this piece of information to enhance their safety program, thus, improving workers' safety and  
856 health. With the performance accuracies of three RNN-based deep learning models in this study,  
857 the best RNN-based deep learning model (i.e., GRU) can learn workers' movement patterns and  
858 provide reliable results for predicting posture-based WMSDs risk. However, it was found that  
859 stooping and overhead working postures were misclassified and could lead to recognition errors.  
860 Nevertheless, the findings of this study can be applied to other work-related risk factors (e.g.,  
861 overexertion, loss of balance events) with specific physical load conditions and reasonable hyper-  
862 parameter tuning through model training and testing, thus, mitigating the risk of developing  
863 WMSDs.

864

### 865 *6.3. Limitations and future research directions*

866 The proposed approach is successful for automated recognition and classification of awkward  
867 working postures in construction. However, there are few limitations and challenges. First, this  
868 study only investigated a small sample of experienced rebar workers and five types of awkward  
869 working postures in construction. With diverse construction workers and physically demanding  
870 construction activities, the small experimental dataset could limit the application of the proposed  
871 approach in the construction industry. Future studies should collect large samples of data from

872 several construction workers (e.g., bricklayers, carpenters) while conducting other types of  
873 awkward working postures (e.g., bending or twisting to lift an object) during a real-world  
874 construction environment. Such dataset with enough samples is crucial in training, testing, and  
875 developing a generalized model for different construction activities. Second, this study considered  
876 limited types of wearable sensor data—plantar pressure data—for automated recognition of  
877 awkward working posture. Notably, there are other types of body sensor networks or wearable  
878 biosensors for collecting heart rate, respiration, and body temperature data could be integrated to  
879 enhance automated monitoring and recognition applications. As such, future research should  
880 include other types of biosensor data. Third, the current study employed only three types of RNN-  
881 based deep learning models for awkward posture recognition and classification. Although useful,  
882 RNN-based deep learning models are specifically designed to handle sequential data, but they  
883 suffer from the vanishing/exploding gradient problem. As a result, RNNs fail to deal with long  
884 sequences if *tanh* is applied as the activation function, whereas the model is unstable if a rectified  
885 linear unit (*relu*) is used (Dang et al., 2020). In addition, RNN layers cannot be stacked into a very  
886 deep model because the saturated activation functions cause the gradient to decay over layers.  
887 Consequently, future research could evaluate other types of deep learning networks (e.g., CNN)  
888 or integrate two or more deep learning networks (e.g., CNN-LSTM) for awkward posture  
889 recognition.

890

## 891 **7. Conclusions**

892 This research evaluates a novel approach of using deep learning-based networks and wearable  
893 insole sensor data to automatically recognize and classify different types of awkward working  
894 postures in construction, which may lead workers to develop WMSDs. Five different types of

895 awkward working postures (i.e., overhead working, squatting, stooping, semi-squatting, and one-  
896 legged kneeling) were conducted, and plantar pressure data were captured by using a wearable  
897 insole pressure system. The classification performance of three RNN-based deep learning  
898 models—LSTM, Bi-LSTM, and GRU— was evaluated using metrics such as accuracy, precision,  
899 recall, specificity, and F1-score. The experimental results show that GRU model outperforms the  
900 other RNN-based deep learning models with a high accuracy of 99.01% and F1-score between  
901 93.19% and 99.39%. These results suggest that GRU model, widely applied for the classification  
902 of time-series and sequential data, can be employed to learn sequential plantar pressure patterns  
903 captured by a wearable insole system to recognize and classify different types of awkward working  
904 postures. The proposed approach will contribute to real-time wearable insole sensor computing by  
905 deploying the performance of GRU model for awkward working posture recognition on  
906 construction sites. In addition, it contributes to automated WMSDs risk recognition among  
907 construction workers by enabling safety managers to continuously monitor awkward working  
908 postures, thus improving workers' safety and health conditions. To develop a detailed practical  
909 guideline for this application, future research could integrate other types of wearable biosensors  
910 (e.g., heart rate monitors) and deep learning networks (e.g., CNN) for vigorous recognition of  
911 awkward working postures.

912

### 913 **Data availability statement**

914 The datasets used in this study are available from the corresponding author upon request.

915

### 916 **Declaration of competing interest**

917 None

918 **Acknowledgement**

919 The authors acknowledged supports from (1) Aston Institute for Urban Technology and the  
920 Environment (ASTUTE), Seedcorn Grants Proposal 2020/21 entitled “Wearable Insole Sensor  
921 Data and a Deep Learning Network-Based Recognition for Musculoskeletal Disorders Prevention  
922 in Construction” and (2) Aston Research and Knowledge Exchange Pump Priming Fund 2021/22  
923 on a Grant Proposal entitled “Digital Twin-Enabled Wearable Sensing Technologies for Improved  
924 Workers’ Activity Recognition and Work-Related Risk Assessment”. Special thanks to all our  
925 participants involved in this study.

926

927 **References**

- 928 Akhavian, R., and Behzadan, A. H. (2016) Smartphone-based construction workers' activity  
929 recognition and classification. *Automation in Construction*, Vol. 71, No. 2, pp. 198–209.  
930 DOI: <https://doi.org/10.1016/j.autcon.2016.08.015>.
- 931 Alawneh, L., Alsarhan, T., Al-Zinati, M., Al-Ayyoub, M., Jararweh, Y., and Lu, H. (2021)  
932 Enhancing human activity recognition using deep learning and time series augmented  
933 data. *Journal of Ambient Intelligence and Humanized Computing*, pp. 1-16. DOI:  
934 <https://doi.org/10.1007/s12652-020-02865-4>.
- 935 Alwasel, A., Abdel-Rahman, E. M., Haas, C. T., and Lee, S. (2017) Experience, productivity, and  
936 musculoskeletal injury among masonry workers. *Journal of Construction Engineering and  
937 Management*, Vol. 143, No. 6, pp. 05017003. DOI:  
938 [https://doi.org/10.1061/\(ASCE\)CO.1943-7862.0001308](https://doi.org/10.1061/(ASCE)CO.1943-7862.0001308).
- 939 Antwi-Afari, M. F., and Li, H. (2018g) Fall risk assessment of construction workers based on  
940 biomechanical gait stability parameters using wearable insole pressure system. *Advanced  
941 Engineering Informatics*, Vol. 38, pp. 683-694. DOI:  
942 <https://doi.org/10.1016/j.aei.2018.10.002>.
- 943 Antwi-Afari, M. F., Li, H., Edwards, D. J., Pärn, E. A., Owusu-Manu, D., Seo, J., and Wong, A.  
944 Y. L. (2018a) Identification of potential biomechanical risk factors for low back disorders  
945 during repetitive rebar lifting. *Construction Innovation*, Vol. 18, No. 2. DOI:  
946 <https://doi.org/10.1108/CI-05-2017-0048>.
- 947 Antwi-Afari, M. F., Li, H., Seo, J., and Wong, A. Y. L. (2018e) Automated detection and  
948 classification of construction workers’ loss of balance events using wearable insole  
949 pressure sensors. *Automation in Construction*, Vol. 96, pp. 189-199. DOI:  
950 <https://doi.org/10.1016/j.autcon.2018.09.010>.
- 951 Antwi-Afari, M. F., Li, H., Umer, W., Yu, Y., and Xing, X. (2020a) Construction activity  
952 recognition and ergonomic risk assessment using a wearable insole pressure system.  
953 *Journal of Construction Engineering and Management*, Vol. 146, No. 7, pp. 04020077.  
954 DOI: [https://doi.org/10.1061/\(ASCE\)CO.1943-7862.0001849](https://doi.org/10.1061/(ASCE)CO.1943-7862.0001849).

955 Antwi-Afari, M. F., Li, H., Wong, J. K W., Oladinrin, O., Ge, J. X., Seo, J., and Wong, A. Y. L.  
956 (2019a) Sensing and warning based technology applications to improve occupational  
957 health and safety in the construction industry: A Literature Review. *Engineering,*  
958 *Construction and Architectural Management*, Vol. 26, No. 8, pp. 1534-1552. DOI:  
959 <https://doi.org/10.1108/ECAM-05-2018-0188>.

960 Antwi-Afari, M. F., Li, H., Yu, Y., and Kong, L. (2018f) Wearable insole pressure system for  
961 automated detection and classification of awkward working postures in construction  
962 workers. *Automation in Construction*, Vol. 96, pp. 433-441. DOI:  
963 <https://doi.org/10.1016/j.autcon.2018.10.004>.

964 Anwer, S., Li, H., Antwi-Afari, M. F., and Wong, A. L. Y. (2021) Associations between physical  
965 or psychosocial risk factors and work-related musculoskeletal disorders in construction  
966 workers based on literature in the last 20 years: A systematic review. *International Journal*  
967 *of Industrial Ergonomics*, Vol. 83, pp. 103113. DOI:  
968 <https://doi.org/10.1016/j.ergon.2021.103113>.

969 Anwer, S., Li, H., Antwi-Afari, M. F., Umer, W., Mehmood, I., Al-Hussein, M., and Wong, A. Y.  
970 L. (2021) Test-retest reliability, validity, and responsiveness of a textile-based wearable  
971 sensor for real-time assessment of physical fatigue in construction bar benders. *Journal of*  
972 *Building Engineering*, Vol. 44, pp. 103348. DOI:  
973 <https://doi.org/10.1016/j.jobe.2021.103348>.

974 Attal, F., Mohammed, S., Dedabrishvili, M., Chamroukhi, F., Oukhellou, L., and Amirat, Y. (2015)  
975 Physical human activity recognition using wearable sensors. *Sensors*, Vol. 15, No. 12, pp.  
976 31314-31338. DOI: <https://doi.org/10.3390/s151229858>.

977 Bao, L., and Intille, S. S. (2004) Activity recognition from user-annotated acceleration data.  
978 In *International Conference on Pervasive Computing*, pp. 1-17, Springer, Berlin,  
979 Heidelberg. DOI: [https://doi.org/10.1007/978-3-540-24646-6\\_1](https://doi.org/10.1007/978-3-540-24646-6_1).

980 Buchholz, B., Paquet, V., Wellman, H. and Forde, M. (2003) Quantification of ergonomic hazards  
981 for ironworkers performing concrete reinforcement tasks during heavy highway  
982 construction. *American Industrial Hygiene Association Journal*, Vol. 64, No. 2, pp. 243-  
983 250. DOI: <http://dx.doi.org/10.1080/15428110308984814>.

984 Caldas, C. H., Torrent, D. G., and Haas, C. T. (2006) Using global positioning system to improve  
985 materials-locating processes on industrial projects. *Journal of Construction Engineering*  
986 *and Management*, Vol. 132, No. 7, pp. 741-749. DOI:  
987 [https://doi.org/10.1061/\(ASCE\)0733-9364\(2006\)132:7\(741\)](https://doi.org/10.1061/(ASCE)0733-9364(2006)132:7(741)).

988 Center for Construction Research and Training (CPWR) (2018) *The Construction Chart*  
989 *Book: The United States Construction Industry and Its Workers*, sixth edition, Silver  
990 Spring, MD 20910. Available at: [https://www.cpwr.com/wp-](https://www.cpwr.com/wp-content/uploads/publications/The_6th_Edition_Construction_eChart_Book.pdf)  
991 [content/uploads/publications/The\\_6th\\_Edition\\_Construction\\_eChart\\_Book.pdf](https://www.cpwr.com/wp-content/uploads/publications/The_6th_Edition_Construction_eChart_Book.pdf) (Accessed:  
992 August 2021).

993 Chen, J., Qiu, J., and Ahn, C. (2017) Construction worker's awkward posture recognition through  
994 supervised motion tensor decomposition. *Automation in Construction*, Vol. 77, pp. 67-81.  
995 DOI: <https://doi.org/10.1016/j.autcon.2017.01.020>.

996 Chen, Y., and Shen, C. (2017) Performance analysis of smartphone-sensor behavior for human  
997 activity recognition. *IEEE Access*, Vol. 5, pp. 3095-3110. DOI:  
998 <https://doi.org/10.1109/ACCESS.2017.2676168>.

999 Dang, L. M., Min, K., Wang, H., Piran, M. J., Lee, C. H., and Moon, H. (2020) Sensor-based and  
1000 vision-based human activity recognition: A comprehensive survey. *Pattern*  
1001 *Recognition*, Vol. 108, pp. 107561. DOI: <https://doi.org/10.1016/j.patcog.2020.107561>.

1002 David, G. C. (2005) Ergonomic methods for assessing exposure to risk factors for work-related  
1003 musculoskeletal disorders. *Occupational Medicine*, Vol. 55, No. 3, pp. 190–199. DOI:  
1004 <https://doi.org/10.1093/occmed/kqi082>.

1005 De Dominicis, C. M., Depari, A., Flammini, A., Rinaldi, S., and Sisinni, E. (2013) Smartphone  
1006 based localization solution for construction site management. In *2013 IEEE Sensors*  
1007 *Applications Symposium Proceedings*, pp. 43-48. DOI:  
1008 <https://doi.org/10.1109/SAS.2013.6493554>.

1009 Delrobaei, M., Memar, S., Pieterman, M., Stratton, T. W., McIsaac, K., and Jog, M. (2018)  
1010 Towards remote monitoring of Parkinson’s disease tremor using wearable motion capture  
1011 systems. *Journal of the Neurological Sciences*, Vol. 384, pp. 38-45. DOI:  
1012 <https://doi.org/10.1016/j.jns.2017.11.004>.

1013 Fang, Q., Li, H., Luo, X., Ding, L., Luo, H., Rose, T. M., and An, W. (2018) Detecting non-  
1014 hardhat-use by a deep learning method from far-field surveillance videos. *Automation in*  
1015 *Construction*, Vol. 85, pp. 1-9. DOI: <https://doi.org/10.1016/j.autcon.2017.09.018>.

1016 Fang, W., Ding, L., Luo, H., and Love, P. E. (2018) Falls from heights: A computer vision-based  
1017 approach for safety harness detection. *Automation in Construction*, Vol. 91, pp. 53-61.  
1018 DOI: <https://doi.org/10.1016/j.autcon.2018.02.018>.

1019 Gers, F. A., Schraudolph, N. N., and Schmidhuber, J. (2002) Learning precise timing with LSTM  
1020 recurrent networks. *Journal of Machine Learning Research*, Vol. 3, No. 1, pp. 115-143.  
1021 Available via:  
1022 [https://search.ebscohost.com/login.aspx?direct=true&db=bth&AN=9793888&site=eds-](https://search.ebscohost.com/login.aspx?direct=true&db=bth&AN=9793888&site=eds-live)  
1023 [live](https://search.ebscohost.com/login.aspx?direct=true&db=bth&AN=9793888&site=eds-live) (Accessed: October 2021).

1024 Gibb, A., Drake, C. and Jones, W. (2018) Costs of occupational ill-health in construction. London:  
1025 Institution of Civil Engineers. Available via:  
1026 [https://www.ice.org.uk/ICEDevelopmentWebPortal/media/Documents/ Disciplines%20and%20Resources/Briefing%20Sheet/ Costs-of-occupational-ill-health-in-](https://www.ice.org.uk/ICEDevelopmentWebPortal/media/Documents/ Disciplines%20and%20Resources/Briefing%20Sheet/ Costs-of-occupational-ill-health-in- constructionformattedFINAL.pdf)  
1027 [constructionformattedFINAL.pdf](https://www.ice.org.uk/ICEDevelopmentWebPortal/media/Documents/ Disciplines%20and%20Resources/Briefing%20Sheet/ Costs-of-occupational-ill-health-in- constructionformattedFINAL.pdf) (Accessed: August 2021).

1029 Goodrum, P. M., McLaren, M. A., and Durfee, A. (2006) The application of active radio frequency  
1030 identification technology for tool tracking on construction job sites. *Automation in*  
1031 *Construction*, Vol. 15, No. 3, pp. 292-302. DOI:  
1032 <https://doi.org/10.1016/j.autcon.2005.06.004>.

1033 Guo, H., Yu, Y., and Skitmore, M. (2017) Visualization technology-based construction safety  
1034 management: a review. *Automation in Construction*, Vol. 73, pp. 135–144. DOI:  
1035 <http://dx.doi.org/10.1016/j.autcon.2016.10.004>.

1036 Han, S., and Lee, S. (2013) A vision-based motion capture and recognition framework for  
1037 behavior-based safety management. *Automation in Construction*. Vol. 35, pp. 131–141.  
1038 DOI: <http://dx.doi.org/10.1016/j.autcon.2013.05.001>.

1039 Health and Safety Executive (HSE) (2020) Construction Statistics in Great Britain, 2020.  
1040 Available via: <https://www.hse.gov.uk/statistics/industry/construction.pdf>. (Accessed:  
1041 August 2021).

1042 Hignett, S., and McAtamney, L. (2000) Rapid entire body assessment (REBA). *Applied*  
1043 *Ergonomics*, Vol. 31, No. 2, pp. 201–205. DOI: [http://dx.doi.org/10.1016/S0003-6870](http://dx.doi.org/10.1016/S0003-6870(99)00039-3)  
1044 [\(99\)00039-3](http://dx.doi.org/10.1016/S0003-6870(99)00039-3).

1045 Hochreiter, S., and Schmidhuber, J. (1997) Long short-term memory. *Neural Computation*, Vol.  
1046 9, No. 8, pp. 1735-1780. DOI: <https://doi.org/10.1162/neco.1997.9.8.1735>.

1047 Ijjina, E. P., and Chalavadi, K. M. (2017) Human action recognition in RGB-D videos using  
1048 motion sequence information and deep learning. *Pattern Recognition*, Vol. 72, pp. 504-516.  
1049 DOI: <https://doi.org/10.1016/j.patcog.2017.07.013>.

1050 Inoue, M., Inoue, S., and Nishida, T. (2018) Deep recurrent neural network for mobile human  
1051 activity recognition with high throughput. *Artificial Life and Robotics*, Vol. 23, No. 2, pp.  
1052 173-185. DOI: <https://doi.org/10.1007/s10015-017-0422-x>.

1053 International Organization for Standardization (ISO) (2006) Ergonomics evaluation of static  
1054 working postures, ISO 11226: 2000, Geneva. Available via:  
1055 <https://www.evs.ee/products/iso-11226-2000> (Accessed: August 2021).

1056 Joshua, L., and Varghese, K. (2010) Accelerometer-based activity recognition in  
1057 construction. *Journal of Computing in Civil Engineering*, Vol. 25, No. 5, pp. 370-379. DOI:  
1058 [https://doi.org/10.1061/\(ASCE\)CP.1943-5487.0000097](https://doi.org/10.1061/(ASCE)CP.1943-5487.0000097).

1059 Karwowski, W. (2001) International encyclopedia of ergonomics and human factors, 2<sup>nd</sup> Edition,  
1060 Vol. 3, CRC Press, LLC. ISBN: 9780415304306.

1061 Kim, K., and Cho, Y. K. (2020) Effective inertial sensor quantity and locations on a body for deep  
1062 learning-based worker's motion recognition. *Automation in Construction*, Vol. 113, pp.  
1063 103126. DOI: <https://doi.org/10.1016/j.autcon.2020.103126>.

1064 Kingma, D. P., and Ba, J. (2014) Adam: A method for stochastic optimization. *arXiv preprint*  
1065 *arXiv:1412.6980*. Available via: <http://arxiv.org/abs/1412.6980> (Accessed: October 2021).

1066 Kivi, P., and Mattila, M. (1991) Analysis and improvement of work postures in the building  
1067 industry: application of the computerised OWAS method. *Applied Ergonomics*, Vol. 22,  
1068 No. 1, pp. 43–48. DOI: [https://doi.org/10.1016/0003-6870\(91\)90009-7](https://doi.org/10.1016/0003-6870(91)90009-7).

1069 Lee, H., Yang, K., Kim, N., and Ahn, C. R. (2020) Detecting excessive load-carrying tasks using  
1070 a deep learning network with a Gramian Angular Field. *Automation in Construction*, Vol.  
1071 120, pp. 103390. DOI: <https://doi.org/10.1016/j.autcon.2020.103390>.

1072 Lee, J., Joo, H., Lee, J., and Chee, Y. (2020) Automatic classification of squat posture using inertial  
1073 sensors: Deep learning approach. *Sensors*, Vol. 20, No. 2, pp. 361. DOI:  
1074 <https://doi.org/10.3390/s20020361>.

1075 Li, H., Shrestha, A., Heidari, H., Le Kernec, J., and Fioranelli, F. (2019). Bi-LSTM network for  
1076 multimodal continuous human activity recognition and fall detection. *IEEE Sensors*  
1077 *Journal*, Vol. 20, No. 3, pp. 1191-1201. DOI: <https://doi.org/10.1109/JSEN.2019.2946095>.

1078 Mantyjarvi, J., Himberg, J., and Seppanen, T. (2001) Recognizing human motion with multiple  
1079 acceleration sensors. In 2001 IEEE International Conference on Systems, Man and  
1080 Cybernetics. E-systems and E-man for Cybernetics in Cyberspace (cat. no. 01ch37236),  
1081 Vol. 2, pp. 747-752. DOI: <https://doi.org/10.1109/ICSMC.2001.973004>.

1082 Mcatamney, L., and Corlett, N. E. (1993) RULA: A survey method for the investigation of work-  
1083 related upper limb disorders. *Applied Ergonomics*, Vol. 24, No. 2, pp. 91–99. DOI:  
1084 [http://dx.doi.org/10.1016/0003-6870\(93\)90080-S](http://dx.doi.org/10.1016/0003-6870(93)90080-S).

1085 Mekruksavanich, S., and Jitpattanakul, A. (2021) LSTM networks using smartphone data for  
1086 sensor-based human activity recognition in smart homes. *Sensors*, Vol. 21, No. 5, pp. 1636.  
1087 DOI: <https://doi.org/10.3390/s21051636>.

1088 Nath, N. D., Chaspari, T., and Behzadan, A. H. (2018) Automated ergonomic risk monitoring  
1089 using body-mounted sensors and machine learning. *Advanced Engineering*  
1090 *Informatics*, Vol. 38, pp. 514-526. DOI: <https://doi.org/10.1016/j.aei.2018.08.020>.



- 1091 Nguyen, T. N., Lee, S., Nguyen-Xuan, H., and Lee, J. (2019) A novel analysis-prediction approach  
 1092 for geometrically nonlinear problems using group method of data handling. *Computer*  
 1093 *Methods in Applied Mechanics and Engineering*, Vol. 354, pp. 506-526. DOI:  
 1094 <https://doi.org/10.1016/j.cma.2019.05.052>.
- 1095 Ordóñez, F. J., and Roggen, D. (2016) Deep convolutional and LSTM recurrent neural networks  
 1096 for multimodal wearable activity recognition. *Sensors*, Vol. 16, No. 1, pp. 115. DOI:  
 1097 <https://doi.org/10.3390/s16010115>.
- 1098 Portugal, I., Alencar, P., and Cowan, D. (2018) The use of machine learning algorithms in  
 1099 recommender systems: A systematic review. *Expert Systems with Applications*, Vol. 97,  
 1100 pp. 205-227. DOI: <https://doi.org/10.1016/j.eswa.2017.12.020>.
- 1101 Preece, S. J., Goulermas, J. Y., Kenney, L. P., Howard, D., Meijer, K., and Crompton, R. (2009)  
 1102 Activity identification using body-mounted sensors—a review of classification  
 1103 techniques. *Physiological Measurement*, Vol. 30, No. 4, R1–R33. DOI:  
 1104 <https://doi.org/10.1088/0967-3334/30/4/R01>.
- 1105 Rashid, K. M., and Louis, J. (2019) Times-series data augmentation and deep learning for  
 1106 construction equipment activity recognition. *Advanced Engineering Informatics*, Vol. 42,  
 1107 pp. 100944. DOI: <https://doi.org/10.1016/j.aei.2019.100944>.
- 1108 Ray, S. J., and Teizer, J. (2012) Real-time construction worker posture analysis for ergonomics  
 1109 training. *Advanced Engineering Informatics*, Vol. 26, No. 2, pp. 439–455. DOI:  
 1110 <http://dx.doi.org/10.1016/j.aei.2012.02.011>.
- 1111 Ryu, J., Seo, J., Jebelli, H., and Lee, S. (2019) Automated action recognition using an  
 1112 accelerometer-embedded wristband-type activity tracker. *Journal of Construction*  
 1113 *Engineering and Management*, Vol. 145, No. 1, pp. 04018114. DOI:  
 1114 [https://doi.org/10.1061/\(ASCE\)CO.1943-7862.0001579](https://doi.org/10.1061/(ASCE)CO.1943-7862.0001579).
- 1115 Safe Work Australia. (2020) Key work health and safety statistics Australia 2020: Work-related  
 1116 injury fatalities. Available at:  
 1117 [https://www.safeworkaustralia.gov.au/sites/default/files/2020-](https://www.safeworkaustralia.gov.au/sites/default/files/2020-11/Key%20Work%20Health%20and%20Safety%20Stats%202020.pdf)  
 1118 [11/Key%20Work%20Health%20and%20Safety%20Stats%202020.pdf](https://www.safeworkaustralia.gov.au/sites/default/files/2020-11/Key%20Work%20Health%20and%20Safety%20Stats%202020.pdf). (Accessed:  
 1119 August 2021).
- 1120 Seo, J., and Lee, S. (2021) Automated postural ergonomic risk assessment using vision-based  
 1121 posture classification. *Automation in Construction*, Vol. 128, pp. 103725. DOI:  
 1122 <https://doi.org/10.1016/j.autcon.2021.103725>.
- 1123 Seo, J., Starbuck, R., Han, S., Lee, S., and Armstrong, T. J. (2015) Motion data-driven  
 1124 biomechanical analysis during construction tasks on sites. *Journal of Computing in Civil*  
 1125 *Engineering*, Vol. 29, No. 4, pp. B4014005. DOI:  
 1126 [https://doi.org/10.1061/\(ASCE\)CP.1943-5487.0000400](https://doi.org/10.1061/(ASCE)CP.1943-5487.0000400).
- 1127 Seyfioglu, M. S., Özbayoğlu, A. M., and Gürbüz, S. Z. (2018) Deep convolutional autoencoder  
 1128 for radar-based classification of similar aided and unaided human activities. *IEEE*  
 1129 *Transactions on Aerospace and Electronic Systems*, Vol. 54, No. 4, pp. 1709-1723. DOI:  
 1130 <https://doi.org/10.1109/TAES.2018.2799758>.
- 1131 Son, H., Choi, H., Seong, H., and Kim, C. (2019) Detection of construction workers under varying  
 1132 poses and changing background in image sequences via very deep residual  
 1133 networks. *Automation in Construction*, Vol. 99, pp. 27-38. DOI:  
 1134 <https://doi.org/10.1016/j.autcon.2018.11.033>.
- 1135 Srivastava, N., Hinton, G., Krizhevsky, A., Sutskever, I., and Salakhutdinov, R. (2014) Dropout:  
 1136 a simple way to prevent neural networks from overfitting. *The Journal of Machine*

1137 Learning Research, Vol. 15, No. 1, pp. 1929-1958. Available via:  
 1138 <http://jmlr.org/papers/v15/srivastava14a.html> (Accessed: October 2021).

1139 Teizer, J., Caldas, C. H., and Haas, C. T. (2007) Real-time three-dimensional occupancy grid  
 1140 modeling for the detection and tracking of construction resources. *Journal of Construction*  
 1141 *Engineering and Management*, Vol. 133, No. 11, pp. 880-888. DOI:  
 1142 [https://doi.org/10.1061/\(ASCE\)0733-9364\(2007\)133:11\(880\)](https://doi.org/10.1061/(ASCE)0733-9364(2007)133:11(880)).

1143 Umer, W., Antwi-Afari, M. F., Li, H., Szeto, G. P., and Wong, A. Y. L. (2017a) The prevalence  
 1144 of musculoskeletal symptoms in the construction industry: A systematic review and meta-  
 1145 analysis. *International Archives of Occupational and Environmental Health*, Vol. 91, No.  
 1146 2, pp. 125-144. DOI: <https://doi.org/10.1007/s00420-017-1273-4>.

1147 Umer, W., Li, H., Szeto, G. P. Y., and Wong, A. Y. L. (2017b) Identification of biomechanical  
 1148 risk factors for the development of lower-back disorders during manual rebar tying. *Journal*  
 1149 *of Construction Engineering and Management*, Vol. 143, No. 1, pp. 04016080. DOI:  
 1150 [https://doi.org/10.1061/\(ASCE\)CO.1943-7862.0001208](https://doi.org/10.1061/(ASCE)CO.1943-7862.0001208).

1151 Umer, W., Li, H., Yu, Y., Antwi-Afari, M. F., Anwer, S., and Luo, X. (2020) Physical exertion  
 1152 modeling for construction tasks using combined cardiorespiratory and thermoregulatory  
 1153 measures. *Automation in Construction*, Vol. 112, pp. 103079. DOI:  
 1154 <https://doi.org/10.1016/j.autcon.2020.103079>.

1155 Valero, E., Sivanathan, A., Bosché, F., and Abdel-Wahab, M. (2017) Analysis of construction  
 1156 trade worker body motions using a wearable and wireless motion sensor  
 1157 network. *Automation in Construction*, Vol. 83, pp. 48-55. DOI:  
 1158 <https://doi.org/10.1016/j.autcon.2017.08.001>.

1159 Wang, D., Dai, F., and Ning, X. (2015a) Risk assessment of work-related musculoskeletal  
 1160 disorders in construction: state-of-the-art review. *Journal of Construction Engineering and*  
 1161 *Management*, Vol. 141, No. 6, pp. 1–15. DOI: [http://dx.doi.org/10.1061/\(ASCE\)CO.1943-7862.0000979](http://dx.doi.org/10.1061/(ASCE)CO.1943-7862.0000979).

1163 Wang, J., Chen, D., Zhu, M., and Sun, Y. (2021). Risk assessment for musculoskeletal disorders  
 1164 based on the characteristics of work posture. *Automation in Construction*, Vol. 131, pp.  
 1165 103921. DOI: <https://doi.org/10.1016/j.autcon.2021.103921>.

1166 Xing, X., Zhong, B., Luo, H., Rose, T., Li, J., and Antwi-Afari, M. F. (2020) Effects of physical  
 1167 fatigue on the induction of mental fatigue of construction workers: A pilot study based on  
 1168 a neurophysiological approach. *Automation in Construction*, Vol. 120, pp. 103381. DOI:  
 1169 <https://doi.org/10.1016/j.autcon.2020.103381>.

1170 Yan, X., Li, H., Li, A. R., and Zhang, H. (2017) Wearable IMU-based real-time motion warning  
 1171 system for construction workers' musculoskeletal disorders prevention. *Automation in*  
 1172 *Construction*, Vol. 74, pp. 2-11. DOI: <https://doi.org/10.1016/j.autcon.2016.11.007>.

1173 Yang, K., Ahn, C. R., and Kim, H. (2020) Deep learning-based classification of work-related  
 1174 physical load levels in construction. *Advanced Engineering Informatics*, Vol. 45, pp.  
 1175 101104. DOI: <https://doi.org/10.1016/j.aei.2020.101104>.

1176 Yang, S., Yu, X., and Zhou, Y. (2020) LSTM and GRU neural network performance comparison  
 1177 study: Taking Yelp review dataset as an example. In *2020 International Workshop on*  
 1178 *Electronic Communication and Artificial Intelligence (IWEC AI)*, pp. 98-101. DOI:  
 1179 <https://doi.org/10.1109/IWEC AI50956.2020.00027>.

1180 Yang, X., Li, H., Yu, Y., Luo, X., Huang, T., and Yang, X. (2018) Automatic pixel-level crack  
 1181 detection and measurement using fully convolutional network. *Computer-Aided Civil and*

1182 Infrastructure Engineering, Vol. 33, No. 12, pp. 1090-1109. DOI:  
 1183 <https://doi.org/10.1111/mice.12412>.

1184 Yilmaz, A., Javed, O., and Shah, M. (2006) Object tracking: A survey. *ACM Computing Surveys*  
 1185 (CSUR), Vol. 38, No. 4, pp. 13-es. DOI: <https://doi.org/10.1145/1177352.1177355>.

1186 Yu, Y., Umer, W., Yang, X., and Antwi-Afari, M. F. (2021) Posture-related data collection  
 1187 methods for construction workers: A review. *Automation in Construction*, Vol. 124, pp.  
 1188 103538. DOI: <https://doi.org/10.1016/j.autcon.2020.103538>.

1189 Yu, Y., Yang, X., Li, H., Luo, X., Guo, H., and Fang, Q. (2019) Joint-level vision-based ergonomic  
 1190 assessment tool for construction workers. *Journal of Construction Engineering and*  
 1191 *Management*, Vol. 145, No. 5, pp. 04019025. DOI:  
 1192 [https://doi.org/10.1061/\(ASCE\)CO.1943-7862.0001647](https://doi.org/10.1061/(ASCE)CO.1943-7862.0001647).

1193 Zarzycki, K., and Ławryńczuk, M. (2021) LSTM and GRU neural networks as models of  
 1194 dynamical processes used in predictive control: A comparison of models developed for two  
 1195 chemical reactors. *Sensors*, Vol. 21, No. 16, pp. 5625. DOI:  
 1196 <https://doi.org/10.3390/s21165625>.

1197 Zhang, H., Yan, X., and Li, H. (2018) Ergonomic posture recognition using 3D view-invariant  
 1198 features from single ordinary camera. *Automation in Construction*, Vol. 94, pp. 1-10. DOI:  
 1199 <https://doi.org/10.1016/j.autcon.2018.05.033>.

1200 Zhao, J., and Obonyo, E. (2020) Convolutional long short-term memory model for recognizing  
 1201 construction workers' postures from wearable inertial measurement units. *Advanced*  
 1202 *Engineering Informatics*, Vol. 46, pp. 101177. DOI:  
 1203 <https://doi.org/10.1016/j.aei.2020.101177>.

1204 Zhao, J., and Obonyo, E. (2021) Applying incremental Deep Neural Networks-based posture  
 1205 recognition model for ergonomics risk assessment in construction. *Advanced Engineering*  
 1206 *Informatics*, Vol. 50, pp. 101374. DOI: <https://doi.org/10.1016/j.aei.2021.101374>.

1207 Zhong, B., Li, H., Luo, H., Zhou, J., Fang, W., and Xing, X. (2020) Ontology-based semantic  
 1208 modeling of knowledge in construction: classification and identification of hazards implied  
 1209 in images. *Journal of Construction Engineering and Management*, Vol. 146, No. 4, pp.  
 1210 04020013. DOI: [https://doi.org/10.1061/\(ASCE\)CO.1943-7862.0001767](https://doi.org/10.1061/(ASCE)CO.1943-7862.0001767).

1211 Zhong, B., Xing, X., Luo, H., Zhou, Q., Li, H., Rose, T., and Fang, W. (2020) Deep learning-based  
 1212 extraction of construction procedural constraints from construction regulations. *Advanced*  
 1213 *Engineering Informatics*, Vol. 43, pp. 101003. DOI:  
 1214 <https://doi.org/10.1016/j.aei.2019.101003>.